

Ecodesigning and Improving Performance of Plugin Hybrid Electric Vehicle in Rolling Terrain through Multi-Criteria Optimization of Powertrain

Debraj Bhattacharjee*¹, Tamal Ghosh², Prabha Bhola¹, Kristian Martinsen², Pranab Dan¹

¹Rajendra Mishra School of Engineering Entrepreneurship, Indian Institute of Technology Kharagpur, West Bengal, India, 721302

²Department of Manufacturing and Civil Engineering (IVB), Norwegian University of Science and Technology, Gjøvik, Norway

*Corresponding Author

Email: debraj1@iitkgp.ac.in

Address: Rajendra Mishra School of Engineering Entrepreneurship, Indian Institute of Technology Kharagpur, West Bengal, India, 721302

Contact No: +91 8981286272

Acknowledgements

The authors wish to thank the authority of Product Analytic and Modelling Lab (PAM lab), Rajendra Mishra School of Engineering Entrepreneurship, Indian Institute of Technology Kharagpur, for providing the facilities to complete the research work.

Declaration of Conflicting Interests

The author(s) declared no potential conflicts of interest with respect to the research, authorship, and/or publication of this article.

Funding

The author(s) received no financial support for the research, authorship, and/or publication of this article.

Ecodesigning and Improving Performance of Plugin Hybrid Electric Vehicle in Rolling Terrain through Multi-Criteria Optimization of Powertrain

Abstract

This work presents an ecodesigning and operating performance improvement methodology in series-parallel Plugin hybrid electric vehicle (PHEV) in passenger car category, through optimisation of powertrain, considering gradeability overreaching rolling terrain. Designing involves consideration for power of prime movers and the geometric specification governing gear ratio, which is the teeth number. PHEV performance is measured in terms of various output characteristics, such as, fuel economy, emissions, vehicle weight, battery charge, maximum velocity and maximum acceleration etc. and such output indicators comprising both ecodesign and vehicle operating performance attributes, eleven in all, are considered. For optimisation, the design space is generated using NREL, ADVISOR simulator in accordance with Taguchi's method. Multi-criteria optimisation is used to converge the aforesaid output indicators into a single one using TOPSIS, MTOPSIS, Grey Relational Analysis and their surrogate assisted evolutionary algorithm (SAEA) based solutions to select the best from. Such design solutions are tested with UDDS driving cycle for performance analysis; reflecting superiority of SAEA based results. However, best values of output indicators are not from a single solution but are spread over these SAEAs. While, gradability is embedded in the model, its variation as supplemental factor, together with total ownership cost, are included, for extended modelling to ascertain the suitability amongst SAEAs. To extend the test for suitability beyond one driving cycle, also a combined one is formed by integrating two other, namely NEDC and 1015Prius with UDDS. The simulation experiment results from combined driving cycle also indicate preference in favour of MTOPSIS-SAEA model, complying upto 25% gradability for rolling terrain, substantially better than the reference model while also ensuring

savings in fuel cost by about 60% over the entire ownership period besides reduction in greenhouse gas emissions ranging between 18% and 21%. This solution also helps in lightweighting the vehicle by over 6%.

Keywords

Plug-in Hybrid Electric Vehicle, Fuel Economy, Component Sizing, Gradeability, Multi Criteria Decision Making, Surrogate Assisted Evolutionary Algorithm

Introduction

This article deals with the powertrain component sizing, for ecodesign and performance improvement, as it has an effect on the Plug-in Hybrid Electric Vehicle (PHEV) alongside the driving pattern and power management strategy (PMS)^{1,2}. The PHEV powertrain component sizing methods can be categorised as sequential, iterative, bi-level and simultaneous optimisation³. The sequential techniques are adopted in recent studies^{4,5} where after setting the Power Management Strategy (PMS), the powertrain component specifications are determined. Iterative techniques, however, optimises the component sizes based on the convergence pattern of the performance results⁶. In each computation cycle, the component sizes as well as the control laws, are selected in simultaneous optimisation methods^{7,8} which is a tedious approach. In bi-level method, nested loops optimisation approach is used to derive the feasible solutions⁹. The PHEV powertrain sizing problem is multi-objective in nature and several studies, which improved the fuel efficiency and emissions (component of eco-design), can be found in published literature. So, only recent important works related to PHEV are discussed here in this section. Zhou, et al., 2017 proposed a Chaos-enhanced Accelerated Particle Swarm Optimization (CAPSO) to find the feasible solutions in powertrain sizing problem (PSP) to increase utilisation of electric drive, with an effective Pareto analysis for the bi-objective problem¹⁰. In another work Zhou, Qin and Hu, 2017 expounded the effect of power flow topology on minimisation of fuel consumption

of both types, fossil and electric¹¹. A series-parallel or power-split PHEV is considered by Chi, Ouyang and Tang, 2017 for design space exploration, where the gear ratios and traction components are optimised using PSO algorithm, for different driving modes¹². Similar study can be found using hybrid optimisation method for multimode PHEV¹³. Multi-objective powertrain sizing brings out a pareto set instead of a single optimal solution due to the problem which is multi-objective in nature¹⁴. Several methodologies have been applied to obtain a single optimal solution from the pareto sets. For example, Millo, et al., 2017 converts the multiple objectives into a single cost function and the CO₂ emission got reduced by 23% and the operating costs by 26%¹⁵. Vehicle cost, efficiency, emission, light-weighting and vehicle life as objective is considered in another similar work¹⁶. Geng, et al., 2018 searched best PHEV transmission configuration which improves fuel economy (FE) around 4% to 10% for three driving cycles while minimising the consumption of fossil fuel and total energy ¹⁷. [Non shorted genetic genetic algorithm are used to find the pareto heads in He et al.,2020 and the desirability function is used for the selection of best solution from the pareto heads¹⁸. Application of neumerical method for powertrain component sizing for connected car can be found in the work of Zulkefli and Sun,2019¹⁹. The powertrain component and crash box optimization for minimum vehicle weight and maximum crash force absorption is presented in Anselma et al.,2020²⁰.](#)

Reducing the engine size and increasing the motor size is a common way to reduce fossil fuel consumption ²¹. Also, improvement in fuel economy (FE) can be achieved by increasing the motor efficiency and reducing the overall vehicle weight²². Along with weight reduction, vehicle operating performance parameters are considered here. The term 'Performance' mentioned here precisely referred to vehicle operating performance like vehicle maximum speed, maximum acceleration, speed error, acceleration error and the capability in covering the target distance as well as performance related to fuel economy and emission attributes under ecodesign category. The use of powertrain cost in PSP can be found in Pourabdollah, et al., 2018 and Angerer

et al.,2018^{23,24}. The studies show a reduction in vehicle weight along with improvement in FE. The component size has effect on the total cost of ownership (TCO), which is an indicator of long-term PHEV benefits, and this can be found in the study of Luján et al., 2016²⁵. Song and his fellow researchers applied Pontryagin minimum principle to optimise the battery pack in a PHEV for improving FE²⁶. Dynamic Programming based optimisation of the hybrid storage system comprising of battery and supercapacitor is recounted by Song et al, 2015²⁷. The optimisation of transmission ratio in PHV for reducing fuel consumption can be found in the study of Guo et al.,2018²⁸. Powertrain component sizing for reducing fuel consumption considering a power management can be found in the study of Madanipour²⁹. Along with all aforementioned factors driving cycle or driving pattern or driving condition plays a crucial role in component sizing. Speeding characteristics define the power demand during driving³⁰. This is the main reason of FE variability in different driving cycles as a distinct driving cycle have unique speeding characteristics³¹. This FE variability can be reduced by combining several driving cycles in a single one³². The driving condition also change the power demand and this can alter the FE. For example, the same driving cycle with various road gradient may produce variation in powertrain component size. Therefore, to develop a potent design, multiple driving cycles with variation in road gradient value need to be consider for checking the suitability of the powertrain and for obtaining a common eco-design of PHEV³³.

Contributions

- This article presents a design methodology that uniquely combined two aspects; one associated with ecodesign and other related to vehicle operating performance, which otherwise to develop a vehicle powertrain model. These two stated aspects, however, were addressed by researcher but in isolation, hence improvement in ecodesign was aimed not factoring in the vehicle operating factors and vice versa.

Hence there has been a need for a design methodology that will consider the trade-offs between these two aspects making the solutions more purpose oriented.

- Furthermore, the vehicle weight a feature not practically considered in earlier model has been incorporated here since this influences the related performance of the vehicle.
- The proposed design especially considers its performance in rolling terrain, where gradeability is upto 25% that addressing a consideration which is truly rare.
- With respect to methodology, the application of MCDM techniques and also hybridising those with Suurrogate Assisted Evolutionary Algorithm for the purpose of optimisation, which is a very new approach.

Plugin Hybrid Electric Vehicle Model

The PHEV powertrain model is portrayed in Figure 1. In this section, the significant components for the PHEV powertrain are illustrated using mathematical models.

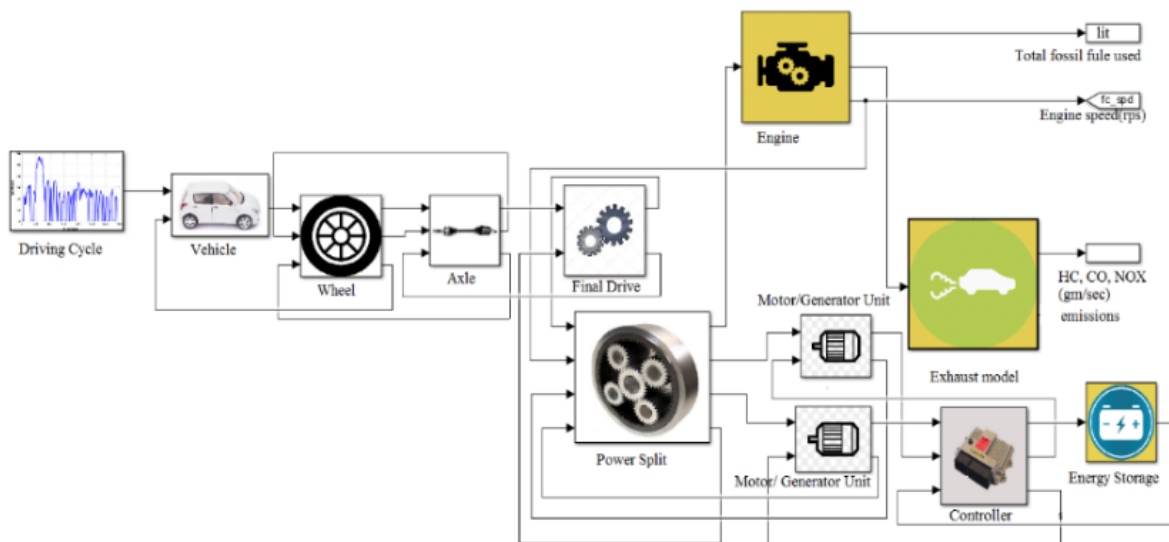


Figure 1. Architecture of the Series-parallel PHEV using MATLAB schematic

Engine Model

The ICE model is composed of maximum power, fuel consumption, Carbon-Monoxide (CO) emission, hydrocarbon (HC) emission and Nitrogen Oxide (NOX) emission models. The engine power (KW) is expressed using Eq. (1).

Where τ_{en} is engine torque and ω_{en} is engine speed. For component sizing, the scale factors are used in this vehicle model. Eq.(2) depicts the engine maximum power as a function of engine torque, speed, and scale factor for the maximum power of the engine.

Where $\epsilon_{en,v}$ is the engine speed scale factor, and $\epsilon_{en,\tau}$ is the engine torque scale factor. The mass of the engine m_{eng} is defined using Eq.(4). The engine inertia J_{en} (Eq.5) is presented as the function of engine power scale factor.

The fuel consumption f_{en} (gram/KW) is portrayed in Eq.(6-7) at a particular moment t .

The emissions (CO, HC, and NOX) are depicted using Eq.(8)-(10).

Electric Motor Model

The mathematical expressions of the electric motor is exhibited using Eq.(11) – (16).

Where τ_{mot} is motor torque and ω_{mot} is motor speed and P_{mot} is motor power.

Where $P_{mt,loss}$ is the power loss, μ_{mt} is the efficiency of the motor. If $P_{mt,in}$ is input power and $P_{mt,o}$ is output power, and $P_{mt,max}$ is the maximum power of the motor then,

The maximum motor power is related to other motor parameters with the scale factor.

Where the motor power scale $_{mt,p}$ is the product of motor angular velocity scale $_{mt,v}$ and motor torque scale $_{mt,\tau}$.

The mass of the motor is also related to maximum motor power with a mass scale factor. The relation could be expressed as,

Generator Model

The mathematical model for generator is expressed using Eq.(17) and Eq.(18)

Where P_{gn} is generator power, τ_{gn} and ω_{gn} are torque and angular velocity of the generator. $P_{gn,tot}$ is the total power for the generator, and μ_{gen} is the engine efficiency. The mass of the vehicle and power is related to scale factors (Eq. 19 - 20).

Battery Model

The battery is modelled using Eq.(21)-(23). The considered model is based on a lithium-ion battery (charge capacity: 6Ah). The mass of the battery module m_{bat} is the function of battery module number N_{bat} .

The state of charge (*SOC*) is defined as the ratio of the remaining charge and maximum charge C_{max} . The model uses the charge used (C_{used}) with current (I), and temperature (T).

Transmission Model

Eq. (24)-(26) presents the HEV transmission or power-split model. The angular velocity and torque distributions are portrayed in Eq. (24) and Eq. (25) respectively. The angular velocity output is ω_{out} , and output torque is τ_{out} .

Where k is the ratio of the ring gear teeth number (N_r) and sun gear teeth number (N_s),

Vehicle Dynamics Model

Based on these components of the powertrain, the vehicle dynamics is presented using Eq.(27)³⁴.

τ_w is the driving torque on the wheel, τ_b is the brake torque, η_o is the final drive efficiency, i_o is the final drive ratio, η_g is the Planetary Gear Set (PGS) efficiency and effecting gear ratio. The acceleration is expressed as,

m_{veh} is the mass of vehicle, g is the gravitational acceleration, C_D is the aerodynamic drag coefficient, θ is the road inclination angle and f_r is the rolling coefficient. The battery power is expressed as,

The overall efficiency of the powertrain is defined as,

The percentage grade is defined as,

More details on the powertrain modeling could be obtained from ref³⁵. In this paper the Toyota Prius series-parallel hybrid architecture is considered as base model, which has the engine power is 43kW, motor power is

31kW, generator power 15 kW, 40 Li-ion battery modules, 78 ring teeth, 30 sun teeth, final drive ratio of 3.93 and vehicle weight of 1320 Kg. The battery used is of 21 Ah battery.

Vehicle Model Validation

For the purpose of validation testing, the vehicle test data of Toyota PRIUS PHEV is retrieved from National Renewable Energy Limited (NREL), which follows SAE J1634 fuel efficiency testing standard³⁶, compared with the vehicle model designed in ADVISOR. The simulation result, based on the present modelling scheme, shows that the fossil fuel mileage value is 38.7 mpg against the laboratory test value of 39.8 mpg and per cent battery capacity used per mile is 2.31 against the laboratory test value of 2.43, which are very close. Therefore, the numerical modelling scheme is regarded as validated.

Methodology

The proposed multi-criteria PHEV powertrain optimisation is performed using three different Multi criteria decision model (MCDM) methods, namely Grey Relational Analysis (GRA), Technique for Order Preference by Similarity (TOPSIS), Modified Technique for Order Preference by Similarity (MTOPSIS) and Assisted Evolutionary Algorithm (SAEA) of these three MCDM models. In these MCDM based methods, eleven responses, namely FE, emission (HC, CO and NOX), state of battery charge, maximum velocity, maximum acceleration, velocity tracking error, acceleration tracking error, failed to travel distance in driving cycle, and vehicle weight, are considered as the design selection criteria, and further total cost of ownership (TCO) and gradeability has been considered as the supplementary factors in the process of best design solution selection. The inclusion of ecodesign parameters and vehicle performance parameters as design criteria formulates the design problem realistic and similar work can be found in the previous work⁴⁷. The initial data are generated using the Design of Experiment (DOE) based on Taguchi's orthogonal array design (OAD). The experiments

are planned on L_{27} table. Figure 2 displays the methodological flowchart for obtaining the best PHEV design. The PHEV powertrain design and PMS are mutually related. This paper has adopted the fuzzy PMS strategies developed in reference³⁷. The PMS flowchart is displayed in Figure 3.

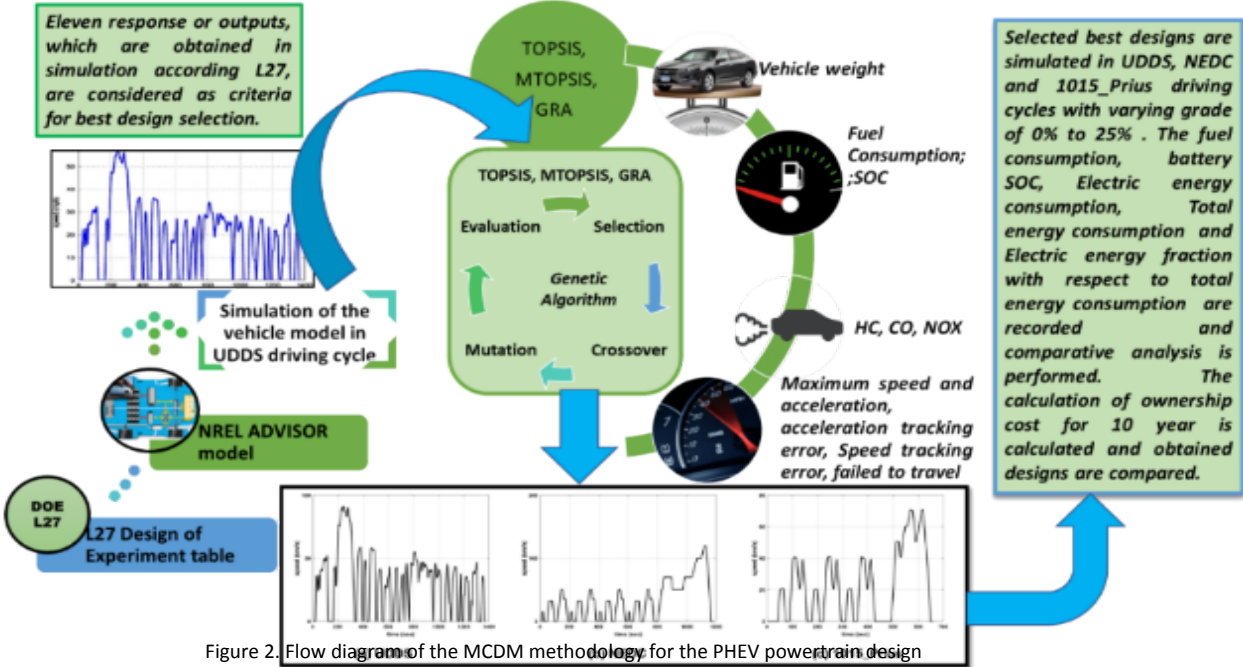


Figure 2. Flow diagram of the MCDM methodology for the PHEV powertrain design

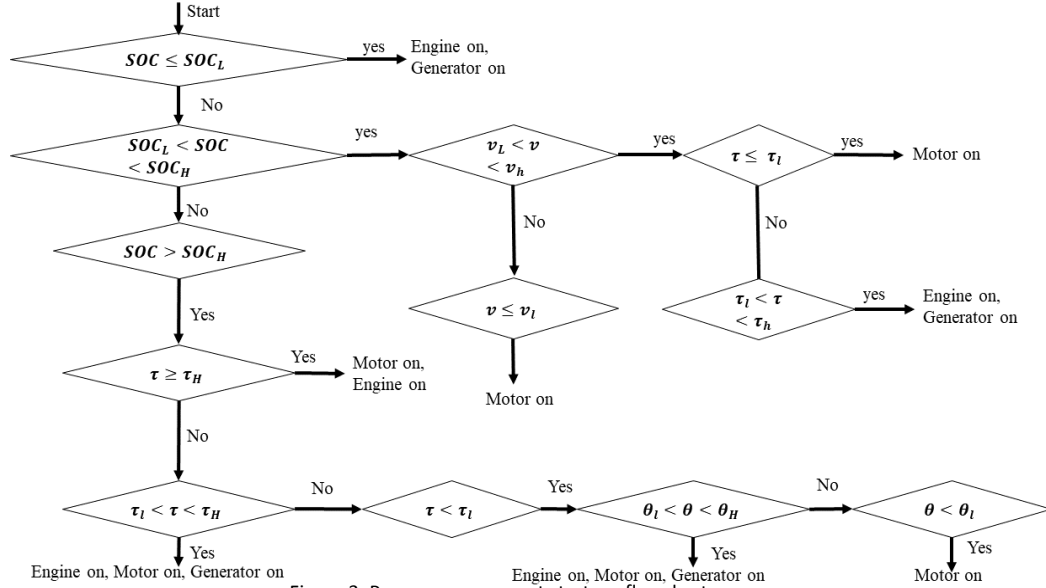


Figure 3. Power management strategy flowchart

GRA Based Technique

Taguchi's OAD is applicable for the single-criteria problem. For MCDM problems, the GRA is suitable³⁸, which has the ability to exploit Taguchi's OAD and estimates the process responses using single grey relational grade (GRG). Steps of GRA are as follows:

Step1: The data are normalised and restricted in the range $\{0, 1\}$. When the performance objective is to be minimised, the non-beneficial (Eq. 32) rule is applied; otherwise, the beneficial (Eq. 33) rule is applied,

Where, $i \in [1, m]$ and $x \in [1, n]$, m is the number of experimental runs and n is the number of responses. $y_i^0(x)_{max}$ and $y_i^0(x)_{min}$ are the largest and smallest values of $y_i^0(x)$ is the original data.

Step2: Compute grey relational coefficient (GRC) using Eq. (34),

Where $\delta_i^0(x) = y_i^0(x) - y_i^*(x)$, the deviation coefficient.

Step3: Calculate GRG using Eq. (35),

GRG depicts the overall quality index, which determines the ranking of experimental runs and obtain a near-optimal set of variables.

TOPSIS Based Technique

The TOPSIS is another MCDM method introduced by reference³⁹ TOPSIS is conceptualised on the select alternatives, which maintain the minimum and maximum Euclidean distances from the Positive Ideal Solution (PIS) and Negative Ideal Solution (NIS) respectively. TOPSIS assigns weights to the criteria, normalise the criteria, and compute the Euclidean distance among the alternatives and ideal solutions. TOPSIS steps are as follows:

Step1: A decision matrix $D = [x_{ij}]_{m \times n}$ is constructed with m alternatives and n criteria, where each element x_{ij} is the performance rating for the alternatives against the criteria.

Step2: The normalisation is done on the decision matrix D using,

Step3: Calculation of the weighted normalised decision matrix is done using,

Where W_j is the weight of j^{th} criteria such that $\sum W_j = 1 \forall j$.

Step4: PIS and NIS are determined using,

where K indicates the beneficial (maximising) criteria and K' indicates the non-beneficial (minimising) criteria.

Step5: The Euclidean distances of each alternative from the PIS and NIS are calculated using Eq. (40) and Eq. (41) respectively.

Step6: Relative closeness calculation is done using,

Where RC_i is the closeness coefficient of i^{th} alternative A_i with respect to the PIS A^+ , $RC_i < 1$; the higher is the RC_i values, better is the rank for the alternatives.

MTOPSIS Based Technique

MTOPSIS is a modified version of the TOPSIS technique based on the synthetic evaluation method⁴⁰. The MTOPSIS method follows similar steps until step 4. Further steps are defined as follows:

Step5: The D^+ and D^- distances are computed, D^+ is considered as the x-axis and D^- is considered as the Y-axis. Therefore, the alternatives could be mapped using (D_i^+, D_i^-) coordinates. A reference point is decided as

the optimal ideal, which is A ($\min(D_i^+)$, $\max(D_i^-)$). Thereafter the distances between each alternative and A is calculated using,

Step 6. The ranking is done using the preference order. Calculation of R_i is done using Eq. (44). The smaller is the R_i value, the better is the ranking score.

On the GRG, TOPSIS, and MTOPSIS performance scores the Taguchi's optimisation can be applied by deriving the Analysis of Variance (ANOVA) to find out the sensitivity of the variables to the design process at 95% confidence level. The response table and main effect plot are obtained. The delta statistic is computed, which shows the difference between the largest and the smallest average for each variable. It finally indicates the most sensitive variables to the design process.

Surrogate Modeling for Design Optimisation

Surrogate assisted model-based engineering design optimisation is a well-known method for finding optimal design solutions from lesser number of experimental or simulation data. In surrogate model, regression, Gaussian process, radial basis function, support vector machines and physics based models are used for product design⁴¹. Some examples of surrogate based models in different sector of engineering design optimisation can be found in references^{42,43,44,45}. In the design of surrogates the use of MCDM models are rare. Here, GRG score (G), TOPSIS score (RC_i) and MTOPSIS score (MRC_i) are considered as surrogate model in Surrogate Assisted Evolutionary Algorithm (SAEA) in powertrain component optimisation.

Genetic Algorithm

Genetic algorithm (GA) is an evolutionary optimisation method for finding the feasible solution. In different application the use of GA can be found for published literatures^{46,47,48}. The application of GA in HEV or electric vehicle can be found in different literatures^{29,49}. The steps of GA is presented below as bullet points.

Step 1: initialise the population size, cross over probability, mutation probability

Step 2: Random generation of the population.

Step 3: Calculate fitness for each solution

Step 4: Select the best solutions

Step 5: crossover and mutation

Step 6: Repeat step 2 to 5 until the stopping criteria reached.

Computational Results

The empirical data for the powertrain are generated using the ADVISOR simulator³⁵ and MATLAB. The design parameters are presented in table 1 and the generated data according to Taguchi's OAD are presented in table 2⁵⁰. The prime objectives are to reduce the fuel cost for an ownership period and gradeability. The design optimisation and selection steps are discussed in this subsection.

Table 1. Design variables and the levels

Variable Name	P_{maxeng}	N_{bat}	P_{maxmot}	P_{maxgen}	N_r	N_s	i_0
Level 1	50	40	50	25	7	3	3.9
Level 2	40	30	40	20	8	0	3
					4	4	0
Level 3	30	20	30	15	5	1	2.5
					0	8	0

Table 2. L₂₇ table for experimental data

No	P_{maxeng}	N_{bat}	P_{maxmot}	P_{maxgen}	N_r	N_s	i_0	m_{veh}	FE	Ea	HC	CO	NOX	E_L	Ev	del_{SOC}	V_{max}	a_{max}
----	--------------	-----------	--------------	--------------	-------	-------	-------	-----------	----	----	----	----	-----	-------	----	-------------	-----------	-----------

1	50	40	50	25	7	3	3.9	121	20.3	5.419	1.36	2.036	0.87	0.0	0.405	0.238	162.	4.7
					8	0	3	7			2		8		4	7	1	
2	50	40	50	25	6	2	3.0	121	28.3	7.209	1.51	2.227	0.90	4.4	0.473	0.242	203.	4.6
					4	4	0	7			0		0		3	2	9	
3	50	40	50	25	5	1	2.5	121	37.1	11.34	2.19	3.178	1.21	7.0	0.572	0.248	203.	3.8
					0	8	0	7		3	2		2		0	6	6	
4	50	30	40	20	7	3	3.9	117	25.6	3.657	1.24	1.866	0.79	2.2	0.317	0.236	162.	4.7
					8	0	3	6			4		7		2	9	1	
5	50	30	40	20	6	2	3.0	117	32.0	9.224	1.80	2.631	1.03	5.7	0.555	0.247	196.	3.8
					4	4	0	6			1		6		9	5	1	
6	50	30	40	20	5	1	2.5	117	44.0	12.91	2.72	3.913	1.45	7.9	0.644	0.248	196.	3.1
					0	8	0	6			9		7		3	9	7	
7	50	20	30	15	7	3	3.9	113	26.9	5.459	1.40	2.072	0.85	3.4	0.547	0.247	162.	3.1
					8	0	3	4			5		4		1	4	8	
8	50	20	30	15	6	2	3.0	113	33.6	10.14	2.01	2.898	1.10	6.2	0.704	0.248	194.	2.6
					4	4	0	4		4	3		7		8	3	9	
9	50	20	30	15	5	1	2.5	113	77.7	16.52	5.87	8.176	2.72	10.	0.774	0.249	193.	2.3
					0	8	0	4		7	1		9		1	3	9	
10	40	40	40	15	7	2	2.5	114	55.7	15.80	3.55	5.142	1.86	9.7	0.647	0.251	218.	3.2
					8	4	0	8		0	2		2		9	1	8	
11	40	40	40	15	6	1	3.9	114	24.9	8.673	1.30	1.958	0.79	5.3	0.490	0.245	161.	4.7
					4	8	3	8			8		5		1	9	8	
12	40	40	40	15	5	3	3.0	114	35.4	10.13	1.59	2.453	1.09	6.2	0.544	0.248	213.	3.8
					0	0	0	8		8	1		4		9	2	4	
13	40	30	30	25	7	2	2.5	114	75.2	16.89	5.05	7.207	2.54	10.	0.734	0.250	206.	2.5
					8	4	0	0		5	6		2		4	1	9	
14	40	30	30	25	6	1	3.9	114	29.1	11.00	1.65	2.443	0.95	6.7	0.567	0.248	162.	4.0
					4	8	3	0		4	4		2		6	7	4	
15	40	30	30	25	5	3	3.0	114	25.1	4.491	1.05	1.651	0.76	2.8	0.395	0.238	162.	3.9
					0	0	0	0			8		3		2	2	6	
16	40	20	50	20	7	2	2.5	115	103.	17.71	7.34	10.35	3.54	10.	0.754	0.250	194.	3.5
					8	4	0	5	5	1	7		4		9	6	1	9
17	40	20	50	20	6	1	3.9	115	27.7	10.68	1.61	2.365	0.91	6.6	0.582	0.249	162.	4.7
					4	8	3	5		2	8		1		9	4	6	
18	40	20	50	20	5	3	3.0	115	25.1	4.976	1.09	1.704	0.77	3.1	0.454	0.241	162.	4.7
					0	0	0	5			9		2		3	9	9	
19	30	40	30	20	7	1	3.0	111	51.1	16.84	3.52	5.181	1.79	10.	0.673	0.250	209.	3.0
					8	8	0	2		6	0		2		3	5	1	6
20	30	40	30	20	6	3	2.5	111	58.0	16.02	2.90	4.419	1.84	9.8	0.704	0.250	203.	2.5
					4	0	0	2		2	0		2		9	0	3	
21	30	40	30	20	5	2	3.9	111	26.5	10.18	1.16	1.819	0.81	6.2	0.542	0.247	162.	3.9
					0	4	3	2		4	0		8		7	5	8	
22	30	30	50	15	7	1	3.0	112	56.1	17.14	3.90	5.603	1.91	10.	0.673	0.251	194.	4.7
					8	8	0	8		8	8		7		5	5	2	7
23	30	30	50	15	6	3	2.5	112	64.2	16.46	3.30	5.028	2.06	10.	0.677	0.249	194.	3.9
					4	0	0	8		6	7		2		1	9	5	0
24	30	30	50	15	5	2	3.9	112	24.7	9.656	1.10	1.722	0.76	5.9	0.536	0.248	162.	4.7
					0	4	3	8			2		8		2	1	8	
25	30	20	40	25	7	1	3.0	111	101.	18.32	7.68	10.74	3.51	11.	0.755	0.250	178.	3.6
					8	8	0	9	6	2	7		9		5	2	6	9
26	30	20	40	25	6	3	2.5	111	99.1	17.64	5.40	8.101	3.22	10.	0.760	0.250	180.	3.0
					4	0	0	9		7	1		8		8	4	9	9
27	30	20	40	25	5	2	3.9	111	28.8	11.52	1.36	2.104	0.91	7.1	0.632	0.248	163.	4.7
					0	4	3	9		6	4		0		6	1	2	

GRA Analysis

The GRA calculations are presented in Table 3. The normalised matrix and the deviation sequences with GRG scores are portrayed in Table 3. The GRA technique converts the MCDM problem into a single objective GRG based problem. Thereafter Taguchi's optimisation is applied on the GRG scores, and the main effect plot for the parameters are portrayed in Figure 4. The near-optimal combination for the parameters would be $P_{maxeng}3-N_{bat}3-P_{maxmot}1-P_{maxgen}2-N_r1-N_s3-i_03$. The analysis of variance (ANOVA) table is depicted in Table 4.

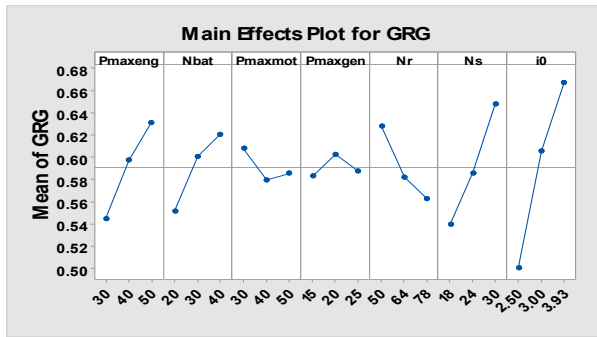


Figure 4. Main effect plot for GRG means

Table 3. Normalised values of responses and deviation sequences

m_v	Normalised Responses										Deviation Sequences										GR G	
	FE	E_a	HC	CO	NO X	E_i	E_v	del_{soc}	V_{max}	a_{max}	FE	E_a	HC	CO	NO X	E_i	E_v	del_{soc}	V_{max}	a_{max}		
0.0	1.0	0.8	0.9	0.9	0.96	1.0	0.8	0.87	0.0	0.0	1.0	0.0	0.1	0.0	0.0	0.04	0.0	0.1	0.13	0.9	1.0	0.74
0	0	8	5	6	0	1	0	1	0	0	0	2	5	4	0	9	9	9	9	0	0	0
0.0	0.9	0.7	0.9	0.9	0.95	0.6	0.6	0.63	0.7	0.0	1.0	0.1	0.2	0.0	0.0	0.05	0.3	0.3	0.37	0.2	0.9	0.66
0	0	6	3	4	1	6	4	4	4	0	0	4	7	6	9	4	6	6	6	6	6	6
0.0	0.8	0.4	0.8	0.8	0.84	0.3	0.4	0.18	0.7	0.3	1.0	0.2	0.5	0.1	0.1	0.16	0.6	0.5	0.82	0.2	0.6	0.56
0	0	8	3	3	8	4	3	8	0	2	7	7	3	6	7	3	6	7	3	7	3	3
0.3	0.9	1.0	0.9	0.9	0.99	0.8	1.0	1.00	0.0	0.0	0.6	0.0	0.0	0.0	0.01	0.2	0.0	0.00	0.9	1.0	0.78	
9	4	0	7	8	0	0	1	0	1	6	0	3	2	0	0	0	9	0	9	0	0	0
0.3	0.8	0.6	0.8	0.8	0.90	0.4	0.4	0.26	0.6	0.3	0.6	0.1	0.3	0.1	0.1	0.10	0.5	0.5	0.74	0.4	0.6	0.61
9	6	2	9	9	9	8	0	8	1	4	8	1	1	1	2	2	0	3	0	3	3	3
0.3	0.7	0.3	0.7	0.7	0.75	0.2	0.2	0.16	0.6	0.6	0.6	0.2	0.6	0.2	0.25	0.7	0.7	0.84	0.3	0.3	0.54	
9	2	7	5	5	9	8	1	7	1	8	3	5	5	1	2	9	3	9	3	3	3	3
0.7	0.9	0.8	0.9	0.9	0.97	0.7	0.5	0.27	0.0	0.6	0.2	0.0	0.1	0.0	0.0	0.03	0.3	0.5	0.73	0.9	0.3	0.69
9	2	8	5	5	0	0	2	7	1	8	2	5	5	0	0	8	3	8	3	8	3	3
0.7	0.8	0.5	0.8	0.8	0.88	0.4	0.1	0.20	0.5	0.8	0.2	0.1	0.4	0.1	0.1	0.12	0.5	0.8	0.80	0.4	0.1	0.63
9	4	6	6	6	5	5	8	8	1	6	4	4	4	4	5	5	2	3	2	3	3	3
0.7	0.3	0.1	0.2	0.2	0.29	0.1	0.0	0.09	0.5	1.0	0.2	0.6	0.8	0.7	0.7	0.71	0.9	1.0	0.91	0.4	0.0	0.48
9	1	2	7	8	0	0	6	0	1	9	8	3	2	0	0	4	0	4	0	4	0	0

0.6	0.5	0.1	0.6	0.6	0.60	0.1	0.2	0.01	1.0	0.6	0.3	0.4	0.8	0.3	0.3	0.40	0.8	0.7	0.99	0.0	0.3	0.54
6	7	7	2	2		3	8		0	3	4	3	3	8	8		7	2		0	8	
0.6	0.9	0.6	0.9	0.9	0.99	0.5	0.6	0.37	0.0	0.0	0.3	0.0	0.3	0.0	0.0	0.01	0.4	0.3	0.63	1.0	1.0	0.65
6	4	6	6	7		3	2		0	0	4	6	4	4	3		7	8		0	0	
0.6	0.8	0.5	0.9	0.9	0.88	0.4	0.5	0.21	0.9	0.3	0.3	0.1	0.4	0.0	0.12	0.5	0.5	0.79	0.0	0.6	0.64	
6	2	6	2	1		5	0		1	8	4	8	4	8	9		5	0		9	3	
0.7	0.3	0.1	0.4	0.3	0.36	0.0	0.0	0.08	0.7	0.9	0.2	0.6	0.9	0.6	0.64	0.9	0.9	0.92	0.2	0.0	0.49	
3	4	0	0	9		7	9		9	2	7	6	0	0	1		3	1		1	8	
0.7	0.8	0.5	0.9	0.9	0.93	0.4	0.4	0.17	0.0	0.2	0.2	0.1	0.5	0.0	0.07	0.6	0.5	0.83	0.9	0.7	0.60	
3	9	0	1	1		0	5		1	9	7	1	0	9	9		0	5		9	1	
0.7	0.9	0.9	1.0	1.0	1.00	0.7	0.8	0.91	0.0	0.3	0.2	0.0	0.0	0.0	0.00	0.2	0.1	0.09	0.9	0.6	0.77	
3	4	4	0	0		5	3		1	3	7	6	6	0	0		5	7		9	7	
0.5	0.0	0.0	0.0	0.0	0.00	0.0	0.0	0.08	0.5	0.5	0.4	1.0	0.9	0.9	0.9	1.00	0.9	0.9	0.92	0.4	0.5	0.39
9	0	4	5	4		3	4		8	0	1	0	6	5	6		7	6		2	0	
0.5	0.9	0.5	0.9	0.9	0.95	0.4	0.4	0.13	0.0	0.0	0.4	0.0	0.4	0.0	0.05	0.5	0.5	0.87	0.9	1.0	0.59	
9	1	2	2	2		1	2		1	0	1	9	8	8	8		9	8		9	0	
0.5	0.9	0.9	0.9	0.9	1.00	0.7	0.7	0.65	0.0	0.0	0.4	0.0	0.0	0.0	0.00	0.2	0.3	0.35	0.9	1.0	0.71	
9	4	1	9	9		2	0		2	0	1	6	9	1	1		8	0		8	0	
1.0	0.6	0.1	0.6	0.6	0.63	0.0	0.2	0.08	0.8	0.7	0.0	0.3	0.9	0.3	0.3	0.37	0.9	0.7	0.92	0.1	0.2	0.56
0	3	0	3	1		8	2		4	1	0	7	0	7	9		2	8		6	9	
1.0	0.5	0.1	0.7	0.7	0.61	0.1	0.1	0.08	0.7	0.9	0.0	0.4	0.8	0.2	0.3	0.39	0.8	0.8	0.92	0.2	0.0	0.57
0	5	6	2	0		3	5		3	2	0	5	4	8	0		8	5		7	8	
1.0	0.9	0.5	0.9	0.9	0.98	0.4	0.5	0.26	0.0	0.3	0.0	0.0	0.4	0.0	0.02	0.5	0.4	0.74	0.9	0.6	0.68	
0	3	5	8	8		5	1		2	3	0	7	5	2	2		5	9		8	7	
0.8	0.5	0.0	0.5	0.5	0.59	0.0	0.2	0.00	0.5	0.0	0.1	0.4	0.9	0.4	0.41	0.9	0.7	1.00	0.4	1.0	0.47	
5	7	8	7	7		6	2		8	0	5	3	2	3	3		4	8		2	0	
0.8	0.4	0.1	0.6	0.6	0.53	0.1	0.2	0.12	0.5	0.3	0.1	0.5	0.8	0.3	0.47	0.9	0.7	0.88	0.4	0.6	0.49	
5	7	3	6	3		0	1		6	3	5	3	7	4	7		0	9		4	7	
0.8	0.9	0.5	0.9	0.9	1.00	0.4	0.5	0.22	0.0	0.0	0.1	0.0	0.4	0.0	0.00	0.5	0.4	0.78	0.9	1.0	0.66	
5	5	9	9	9		7	2		2	0	5	5	1	1	1		3	8		8	0	
0.9	0.0	0.0	0.0	0.0	0.01	0.0	0.0	0.04	0.3	0.4	0.0	0.9	1.0	1.0	1.0	0.99	1.0	0.9	0.96	0.7	0.5	0.41
3	2	0	0	0		0	4		0	6	7	8	0	0	0		0	6		0	4	
0.9	0.0	0.0	0.3	0.2	0.11	0.0	0.0	0.02	0.3	0.7	0.0	0.9	0.9	0.6	0.7	0.89	0.9	0.9	0.98	0.6	0.2	0.44
3	5	5	4	9		4	3		4	1	7	5	5	6	1		6	7		6	9	
0.9	0.9	0.4	0.9	0.9	0.95	0.3	0.3	0.22	0.0	0.0	0.0	0.1	0.5	0.0	0.0	0.05	0.6	0.6	0.78	0.9	1.0	0.62
3	0	6	5	5		7	1		2	0	7	0	4	5	5		3	9		8	0	

Table 4. ANOVA table for GRG

Source	DF	Adj. SS	Adj. MS	F	p	% Contribution
$P_{\max\text{eng}}$	1	0.03389	0.03389	15.02	0.001	11.78%
N_{bat}	1	0.02142	0.02142	9.49	0.006	7.44%
$P_{\max\text{mot}}$	1	0.00228	0.00228	1.01	0.328	0.79%
$P_{\max\text{gen}}$	1	0.00011	0.00011	0.05	0.83	0.04%
N_f	1	0.01927	0.01927	8.54	0.009	6.7%
N_s	1	0.05259	0.05259	23.31	0	18.28%
i_0	1	0.11529	0.11529	51.1	0	40.07%
Error	19	0.04287	0.00226			
Total	26	0.28773				

TOPSIS Analysis

The TOPSIS results are displayed in Table 5-7. The performance scores for the TOPSIS method are depicted in the last column of Table 7.

Table 5. Weighted normalised matrix using TOPSIS

m_v	FE	E_a	HC	CO	NOX	E_L	E_v	del_{SOC}	V_{\max}	a_{\max}
0.01854	0.00679	0.00753	0.00708	0.00736	0.00876	0	0.01164	0.01688	0.01531	0.02136
4	1	8	4	2	5		2	1	1	0
0.01854	0.00946	0.01002	0.00785	0.00805	0.00898	0.01001	0.01359	0.01712	0.01925	0.02090
4	7	8	4	3	5	9	2	8	9	6

0.01854	0.01241	0.01577	0.01140	0.01149	0.01209	0.01593	0.01642	0.01758	0.01923	0.01727
4	1	7	2	2	9	9	4	1	1	0
0.01791	0.00856	0.00508	0.00647	0.00674	0.00795	0.00500	0.00910	0.01675	0.01531	0.02136
9	4	6	1	8	7	9	9	4	1	0
0.01791	0.01070	0.01283	0.00936	0.00951	0.01034	0.01297	0.01596	0.01750	0.01852	0.01727
9	4	0	8	4	2	9	3	3	2	0
0.01791	0.01471	0.01796	0.01415	0.01415	0.01454	0.01798	0.01850	0.01760	0.01857	0.01408
9	9	9	8	0	5	8	1	2	9	9
0.01727	0.00899	0.00759	0.00730	0.00749	0.00852	0.00774	0.01571	0.01749	0.01537	0.01408
9	8	3	8	2	6	2	1	6	7	9
0.01727	0.01124	0.01411	0.01047	0.01047	0.01105	0.01411	0.02024	0.01756	0.01840	0.01181
9		0	1	9	1	7	2	0	9	6
0.01727	0.02599	0.02298	0.03053	0.02956	0.02724	0.02299	0.02223	0.01767	0.01831	0.01045
9	2	9	8	5	4	7	5	3	5	3
0.01749	0.01863	0.02197	0.01847	0.01859	0.01858	0.02208	0.01860	0.01775	0.02066	0.01454
3	2	7	6	4	8	7	6	8	6	3
0.01749	0.00832	0.01206	0.00680	0.00708	0.00793	0.01206	0.01407	0.01739	0.01528	0.02136
3	9	4	3	0	7	8	5	0	3	0
0.01749	0.01184	0.01410	0.00827	0.00887	0.01092	0.01411	0.01564	0.01755	0.02015	0.01727
3	2	2	6	0	1	7	8	3	6	0
0.01737	0.02515	0.02350	0.02629	0.02606	0.02537	0.02368	0.02108	0.01768	0.01954	0.01136
1	6	0	9	1	7	0	1	7	2	2
0.01737	0.00973	0.01530	0.00860	0.00883	0.00950	0.01525	0.01629	0.01758	0.01533	0.01817
1	4	6	3	4	4	6	8	8	9	9
0.01737	0.00839	0.00624	0.00550	0.00597	0.00761	0.00637	0.01134	0.01684	0.01535	0.01772
1	6	6	3	0	7	6	8	6	8	4
0.01759	0.03462	0.02463	0.03821	0.03742	0.03538	0.02481	0.02166	0.01768	0.01840	0.01590
9	2	6	5	6	0	9	8	7	9	7
0.01759	0.00926	0.01485	0.00841	0.00855	0.00909	0.01502	0.01673	0.01763	0.01535	0.02136
9	6	8	6	2	5	8	9	8	8	0
0.01759	0.00839	0.00692	0.00571	0.00616	0.00770	0.00705	0.01304	0.01710	0.01538	0.02136
9	6	1	6	2	7	9	7	7	7	0
0.01694	0.01709	0.02343	0.01830	0.01873	0.01789	0.02345	0.01934	0.01768	0.01979	0.01363
4	4	3	9	5	0	3	0	7	8	4
0.01694	0.01940	0.02228	0.01508	0.01597	0.01838	0.02231	0.02024	0.01768	0.01920	0.01136
4	2	7	4	9	9	4	2	0	2	2
0.01694	0.00886	0.01416	0.00603	0.00657	0.00816	0.01411	0.01558	0.01750	0.01537	0.01772
4	5	6	4	8	6	7	5	3	7	4
0.01718	0.01876	0.02385	0.02032	0.02026	0.01913	0.02390	0.01934	0.01776	0.01839	0.02136
8	6	3	7	1	8	8	0	5	0	0
0.01718	0.02147	0.02290	0.01720	0.01818	0.02058	0.02299	0.01946	0.01764	0.01832	0.01772
8	6	4	1	1	5	7	6	5	4	4
0.01718	0.00826	0.01343	0.00573	0.00622	0.00766	0.01343	0.01539	0.01754	0.01537	0.02136
8	3	1	2	7	7	4	6	6	7	0
0.01705	0.03398	0.02548	0.03998	0.03886	0.03509	0.02550	0.02168	0.01772	0.01689	0.01636
1	7	5	4	9	0	2	9	2	8	1
0.01705	0.03315	0.02454	0.02809	0.02929	0.03222	0.02459	0.02183	0.01774	0.01708	0.01363
1	0	6	3	4	5	1	6	4	7	4
0.01705	0.00963	0.01603	0.00709	0.00760	0.00908	0.01616	0.01816	0.01754	0.01541	0.02136
1	4	2	5	8	5	6	5	6	5	0

Table 6. Ideal best and ideal worst solution calculation

V	0.01694	0.00679	0.00508	0.00550	0.00597	0.00761	0	0.00910	0.016754	0.020666	0.010453
---	---------	---------	---------	---------	---------	---------	---	---------	----------	----------	----------

+	4	1	6	3	7	9				
V-	0.01854	0.03462	0.02548	0.03998	0.03886	0.02550	0.02223	0.017765	0.015283	0.02136
	4	2	5	4	9	2	5			

The Taguchi's analysis is performed on the performance scores RC_i . The main effect plot for TOPSIS performance scores is portrayed in Figure 5. The near-optimal combination for the decision variables would be $P_{maxeng}3-N_{bat}3-P_{maxmot}3-P_{maxgen}2-N_r1-N_s3-i_03$. The ANOVA analysis is depicted in Table 8.

Table 7. Score matrix for TOPSIS

D_i^+	D_i^-	RC_i
0.01297725	0.068142579	0.840024
0.016665385	0.062299201	0.788951
0.02430217	0.053418879	0.687315
0.013360185	0.067791932	0.835369
0.019447618	0.058154792	0.749394
0.029149152	0.047950608	0.621929
0.012764888	0.064518048	0.834829
0.022112949	0.056401151	0.718357
0.054456205	0.021418379	0.282287
0.038335347	0.039051300	0.504626
0.019314372	0.063121308	0.765704
0.020580259	0.058023116	0.738176
0.050349445	0.025866793	0.339387
0.022535501	0.058576196	0.722167
0.011438087	0.067821125	0.855688
0.06926022	0.006865293	0.090184
0.023481122	0.059188187	0.715963
0.014790967	0.066843822	0.818815
0.039263875	0.039846694	0.503684
0.037264019	0.042503304	0.532841
0.020257036	0.062587291	0.755481
0.043055734	0.035678324	0.453150
0.041019665	0.03719738	0.475566
0.020966007	0.063569567	0.751986
0.070995880	0.005533307	0.072303
0.059363494	0.017670142	0.229382
0.025016417	0.059750562	0.704880

Table 8. ANOVA table for TOPSIS performance scores

Source	DF	Adj. SS	Adj. MS	F	p	% Contribution
P_{maxeng}	1	0.19618	0.196185	14.22	0.001	14.03%
N_{bat}	1	0.15121	0.151213	10.96	0.004	10.81%
P_{maxmot}	1	0.00033	0.000331	0.02	0.878	0.02%
P_{maxgen}	1	0.00450	0.004499	0.33	0.575	0.32%
N_r	1	0.16878	0.168781	12.23	0.002	12.07%
N_s	1	0.09919	0.099189	7.19	0.015	7.09%
i_0	1	0.51560	0.515600	37.37	0.000	36.88%
Error	19	0.26216	0.013798			
Total	26	1.39795				

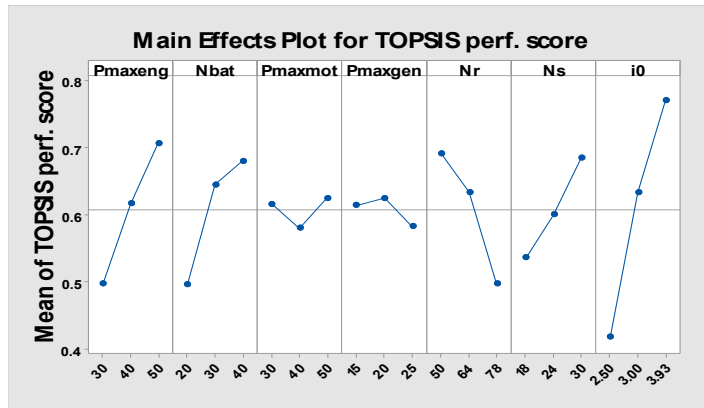


Figure 5: Main effect plot of TOPSIS performance scores

MTOPSIS Analysis

MTOPSIS analysis is similar to the TOPSIS analysis as both the techniques are grounded on the same methodology. MTOPSIS results are displayed in Table 9 (calculated from Table 5-6). The performance scores for this method are depicted in the last column of Table 9. The Taguchi's analysis is performed on the performance scores RC_i . The main effect plot, for MTOPSIS performance scores, is portrayed in Figure 6.

The near-optimal combination for the decision variables would be $P_{\max\text{eng}}3-N_{\text{bat}}3-P_{\max\text{mot}}3-P_{\max\text{gen}}3-N_r3-N_s3-i_03$.

The ANOVA analysis for the MTOPSIS is provided in Table 10.

Table 9. Euclidean distance table for MTOPSIS

D_i^+	D_i^-	MRC_i
0.07360174	0.93162446	0.92678
5	7	1
0.82327700	0.25646660	0.23752
8	0	5
0.86456132	0.19329219	0.18272
2	7	1
0.77105309	0.31394095	0.28934
5	8	8
0.84506927	0.22459912	0.20997
0	1	1
0.87846582	0.16253217	0.15613
3	9	1
0.80235237	0.27674127	0.25645
0	7	7
0.85338775	0.21285317	0.19963
2	0	0
0.92120749	0.07382073	0.07419
3	4	0
0.90247685	0.12147369	0.11863
5	2	2
0.83784572	0.26609601	0.24104
7	5	2
0.85181943	0.22504344	0.20898
6	6	1
0.91951075	0.08129781	0.08123
5	8	2
0.85823185	0.23010216	0.21142
4	9	6
0.78725015	0.31069269	0.28297
7	5	7
0.93914052	0.02838962	0.02934
4	5	2
0.85740998	0.23524929	0.21530
7	1	0
0.79588353	0.30106096	0.27445
8	1	4
0.90709190	0.12554938	0.12158
1	4	1
0.90125903	0.13935012	0.13391
1	2	2
0.85014091	0.26534384	0.23787
1	7	3
0.91269796	0.10613966	0.10417
1	7	7
0.90779882	0.11258144	0.11033
0	6	3
0.84664615	0.27452945	0.24485
7	1	9

Table 10. ANOVA table for MTOPSIS performance scores

Source	DF	Adj. SS	Adj. MS	F	p	% Contribution
$P_{\max\text{eng}}$	1	0.091299	0.091299	8.12	0.010	12.91%
N_{bat}	1	0.062611	0.062611	5.57	0.029	8.85%
$P_{\max\text{mot}}$	1	0.029299	0.029299	2.61	0.123	4.14%
$P_{\max\text{gen}}$	1	0.024379	0.024379	2.17	0.157	3.45%
N_r	1	0.000274	0.000274	0.02	0.878	0.03%
N_s	1	0.080889	0.080889	7.19	0.015	11.44%
i_0	1	0.204542	0.204542	18.19	0.000	28.92%
Error	19	0.213636	0.011244			
Total	26	0.706930				

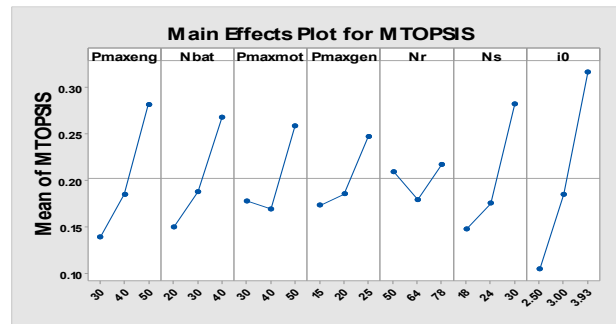


Figure 6. Main effect plot for MTOPSIS performance scores

0.94253832	0.02348655	0.02431
4	0	3
0.93015568	0.05339613	0.05428
9	9	9
0.86343405	0.24278337	0.21947
2	2	2

Design Optimisation Using Surrogate modelling

Here three different regression models are derived from the calculated scores of GRA, TOPSIS and MTOPSIS. In designing a HEV the main contributed of the cost is the power sources in a vehicle powertrain. So, the power split device design is considered constant and therefore, the Ring teeth number and sun teeth number are fixed as 78 and 30. The regression models are presented in table 11. The solution points from the optimisation methods are presented in table 12 along with the base model. The problem formulation for the design optimisation is presented in equation 45.

Table 11. Regression models.

mode <i>l</i>	Constant			<i>Nr</i>			<i>Ns</i>		<i>R</i> ²
GRG	-0.069	0.0044	0.003	-0.0011	0.0004	-0.0023	0.009	0.110	0.8
<i>RC_i</i>	-0.627	0.0104	0.009	0.0043	-0.0032	-0.0069	0.012	0.233	0.8
<i>MRC_i</i>	-1.316	0.0071	0.005	0.0040	0.0074	0.0003	0.011	0.146	0.7
			6				0	8	5
			2				4	2	1
			9				2	9	0

]

St.

Table 12. Solution design points

Method	%Δ	%Δ	<i>kWhr</i>	%Δ	%Δ	%Δ
--------	----	----	-------------	----	----	----

GRAGA	48	11.6	40	0	9.22	40.5	30	-3.2	22	46.7	78	30	3.93
TOPSISGA	49	13.9	39	-2.5	8.99	37.0	45	45.1	18	20.0	78	30	3.93
MTOPSISGA	49	13.9	40	0	9.22	40.5	49	58.1	23	53.3	78	30	3.87
GRA	50	16.3	40	0	9.22	40.5	30	-3.2	25	66.7	50	30	3.93
TOPSIS	50	16.3	40	0	9.22	40.5	50	61.3	20	33.3	50	30	3.93
MTOPSIS	50	16.3	40	0	9.22	40.5	50	61.3	25	66.37	78	30	3.93
Base model(Prius)	43		40		6.56		31		15		78	30	3.93

Performance measurement of obtained design points

The vehicle performances are calculated in UDDS driving cycle with 20% road gradient and presented in table 13. Here vehicle mass (m_v), fuel economy (FE), emissions (HC, CO, NOX), SOC consumption (del_{soc}), Electric energy utilisation (EEU), Total Energy Utilisation (TEU), Wheel torque change (MTC) and cost of powertrain (Cost) are measured for performance comparisons. Here in this work, the powertrain component cost model is considered from a published article⁵¹ and the cost model is presented through equation (46) to (48).

Table 13. Performance analysis and cost analysis in UDDS driving cycle with 20% grade

Method	m_v (kg)	FE (L/100 km)	HC (gm/km)	CO (gm/km)	NOX (gm/km)	del_{soc}	EEU (kJ)	TEU (kJ)	MTC (Nm)	Cost (\$)
GRA	1202	25.5	1.07	1.66	0.77	0.2451	4533.9	55571.5	3317.1	9756
TOPSIS	1239	24.7	1.06	1.66	0.76	0.2154	4478.5	57197.0	3263.6	10082
MTOPSIS	1250	22.1	1.02	1.55	0.68	0.2244	4627.0	54836.4	3203.9	10191
GRA+GA	1200	21.3	0.97	1.48	0.65	0.2342	4735.9	51713.7	3068.9	9666
TOPSIS+GA	1222	21.6	1.00	1.52	0.66	0.2263	4523.1	53274.6	3132.2	9768
MTOPSIS+GA	1241	21.6	1.00	1.51	0.66	0.2308	4668.6	53834.0	3181.4	10114

The vehicle solutions are tested in three different driving cycles. The three driving cycles UDDS, NEDC and 1015_prius are presented in figure 7. The UDDS driving cycle is selected to test vehicle model in highly start

and stop situations. NEDC is selected for testing the vehicle model in both urban and highway testing. Finally the 1015_prius driving cycle is selected as it is used to test the Toyota Prius vehicle.

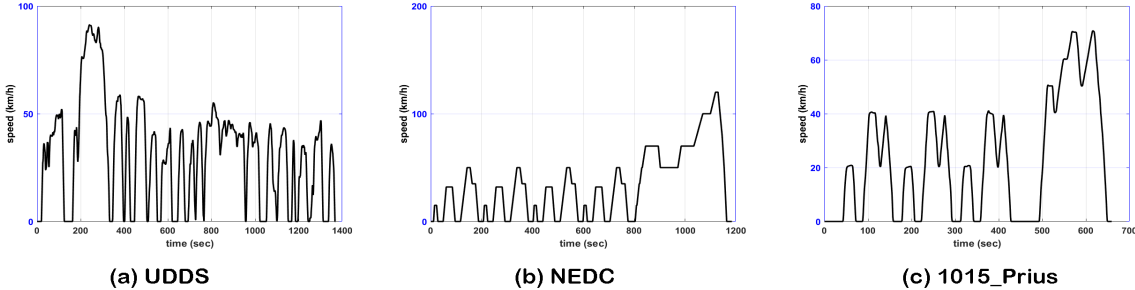


Figure 7. Driving cycles used in analysis (a) UDDS (b) NEDC (c) 1015_Prius

The optimal values of all the eleven output features are distributed over the three solutions, as can be seen in table 13 and therefore no particular solution can be considered as best up till this stage. But in figure 8 it can be seen that the design change leads to improvement in motor operating points and it also found that the average operating efficiency of battery for the three design solutions, namely GRAGA, TOPSISGA and MTOPSISGA, are 91.09% , 92.82% and 93.09%. Which is why, further refinement is necessary and for that other important associated supplemental factors have been explored. An extension model with supplemental factors namely variation in gradeability and TCO, are therefore considered for each driving cycle and presented in a subsequent section ‘Model extension with gradient variability and TCO’.

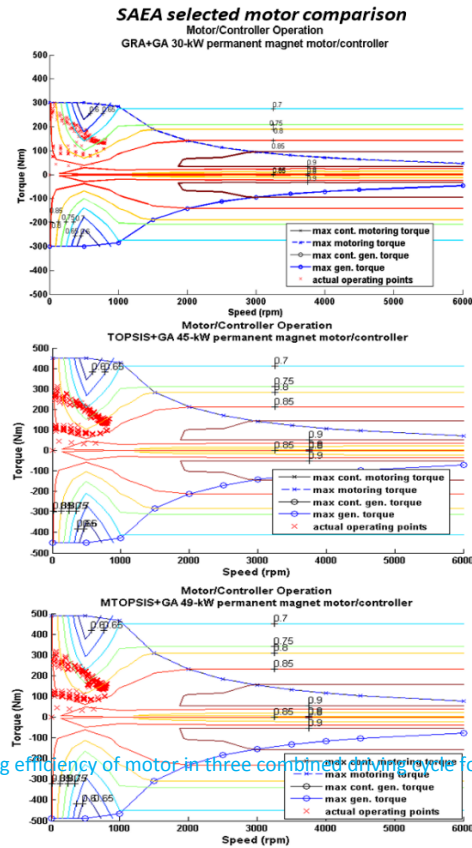


Figure 8. Average operating efficiency of motor in three combined cycle for three design solution

Average operating efficiency of GRA+GA motor is 81.37%, Average operating efficiency of TOPSIS+GA motor is 85.72%, Average operating efficiency of MTOPSIS+GA motor is 86.44%

Model extension with gradient variability and TCO

As just stated in the previous section the two aspects variation in gradeability and TCO (Total cost of Ownership) has been explicated here along with determining the component values and estimation approach. The issue of TCO has already been underscored in the introduction section as well as in the methodology sections under the sub heading ‘Performance measurement of obtained design points’, are being included in the model to extend the same aiming to secure single solution for all practical application purpose as none of the three SAEA solutions contains the best values of the eleven output indicators. Fuel, both fossil (gasoline) and electric type, are cost components which are also major and also variable in nature that constitute TCO besides the other fixed type cost namely Maintenance and repairs, depreciation, Insurance, tax and subsidy.

These fixed type cost and their estimation approach are obtainable from literature and has been used in this work. Therefore, here the task remains, primarily to determine the major variable cost component which effectively are due to gasoline and electric fuel cost, that basically is dependent on the model type or design of the vehicle. The fuel cost actually creates difference as it varies based on the design or vehicle model that is selected. The fuel consumption rate varies with gradeability; that is the consumption pattern needs to be assessed at multiple gradients over each individual driving cycle. Four gradeability values are considered for testing the models based on a design rational; that is, it will cover travelling on plane, to the rolling terrain and a couple of intermediate values. For plane the gradeability is 0% and for the rolling terrain the maximum value for the gradeability is 25%⁵², while for two intermediate values with 10% increment from the plan level (0% gradeability) have been considered. Hence, the consumption of gasoline and electric fuel in this study has been estimated at four gradeability values (0%, 10%, 20% and 25%), which has been worked out using ADVISOR and the generated simulation data regarding such consumption is retrieved where the values are depicted in figures 9 through 12. In figures the prius indicates the base model. The output feature, analysed for individual driving cycle, have been arraigned exclusively for 0%, 10%, and 20% gradeability only to improve legibility of figure 9 through figure 11, where the one of the output features namely electric energy utilisation fraction in table 14, while the data for 25% gradeability is presented separately in figure 12. Though, in effect all these diagrams indicate the performance of the extended model at the four gradeability points only the detail elastration for 25% gradeability as a case example is only presented to economise on space of the present manuscript.

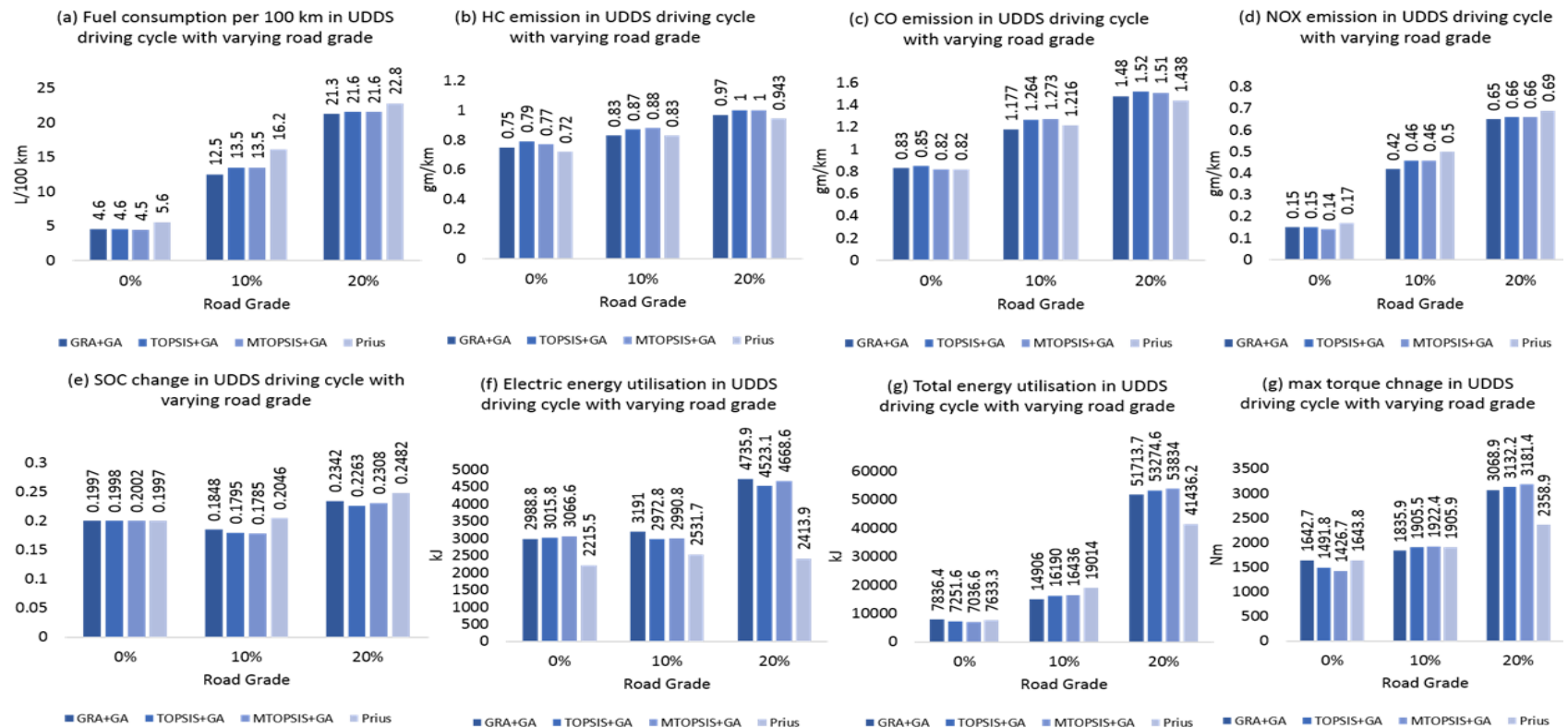


Figure 9. UDDS driving cycle results for varying road grade (a) Fuel consumption (b) HC emission (c) CO emission (d) NOX emission (e) SOC change (f) Electric energy utilisation (g) Total energy utilisation (h) Maximum torque change

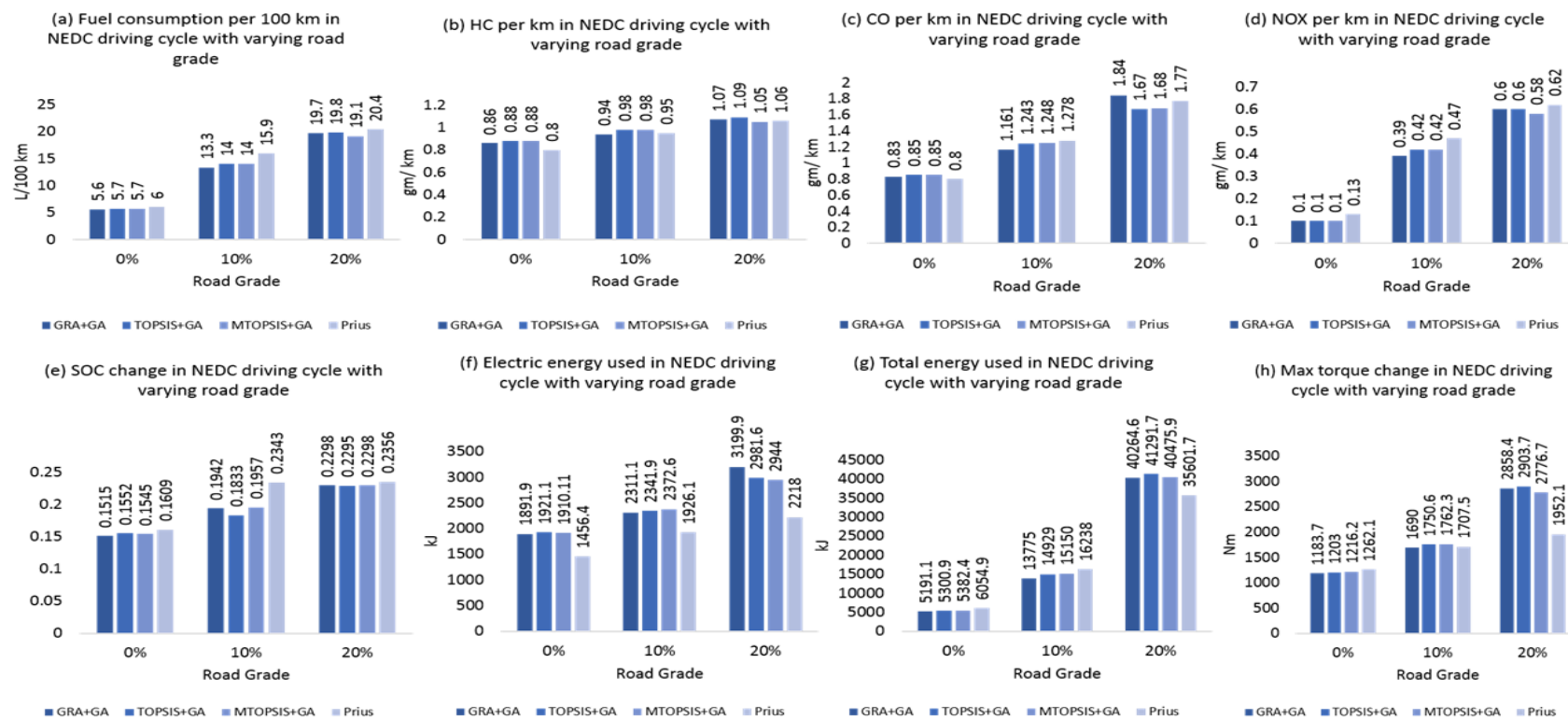


Figure 10. NEDC driving cycle results for varying road grade (a) Fuel consumption (b) HC emission (c) CO emission (d) NOx emission (e) SOC change (f) Electric energy utilisation (g) Total energy utilisation (h) Maximum torque change

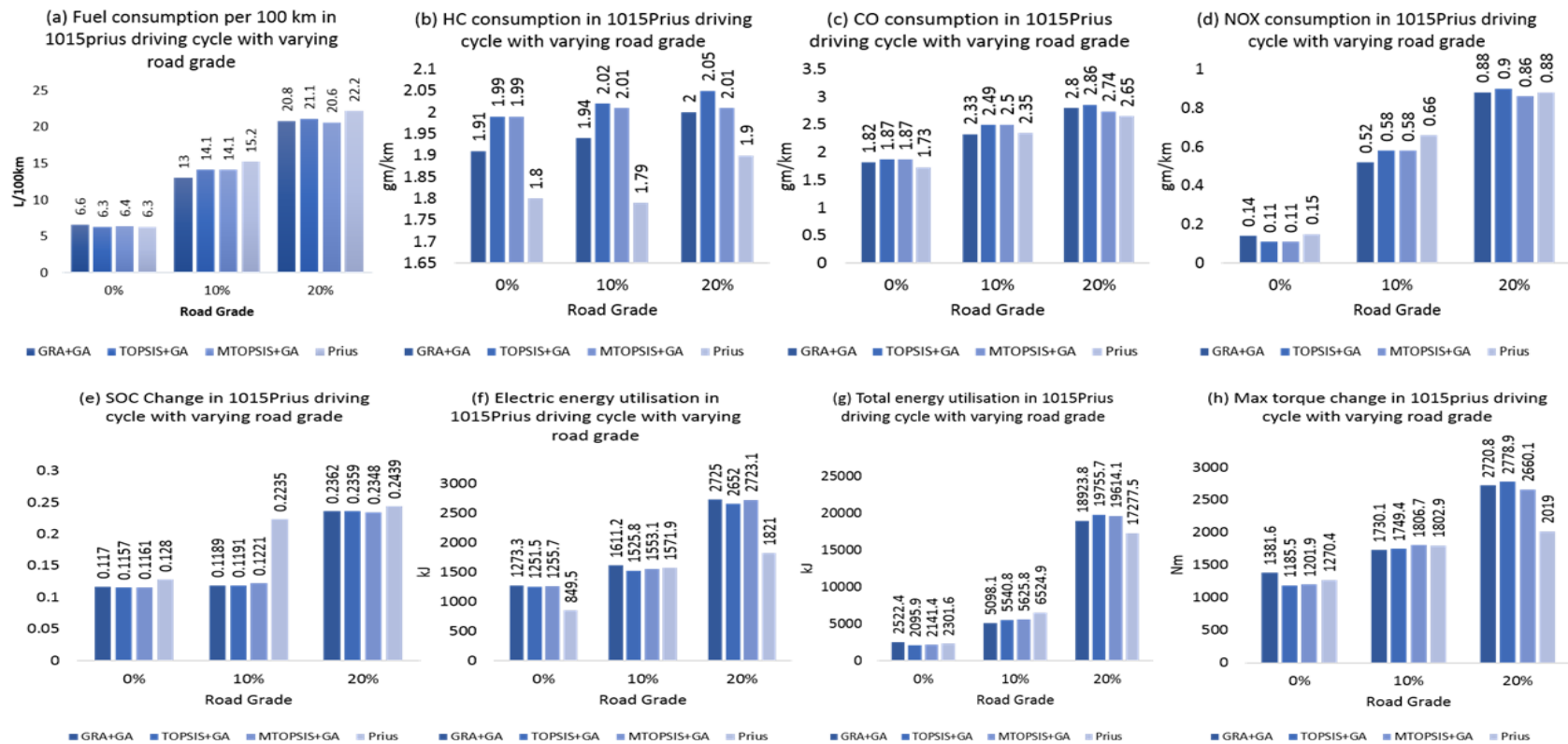


Figure 11.1015_6Prius driving cycle results for varying road grade (a) Fuel consumption (b) HC emission (c) CO emission (d) NOx emission (e) SOC change (f) Electric energy utilisation (g) Total energy utilisation (h) Maximum torque change

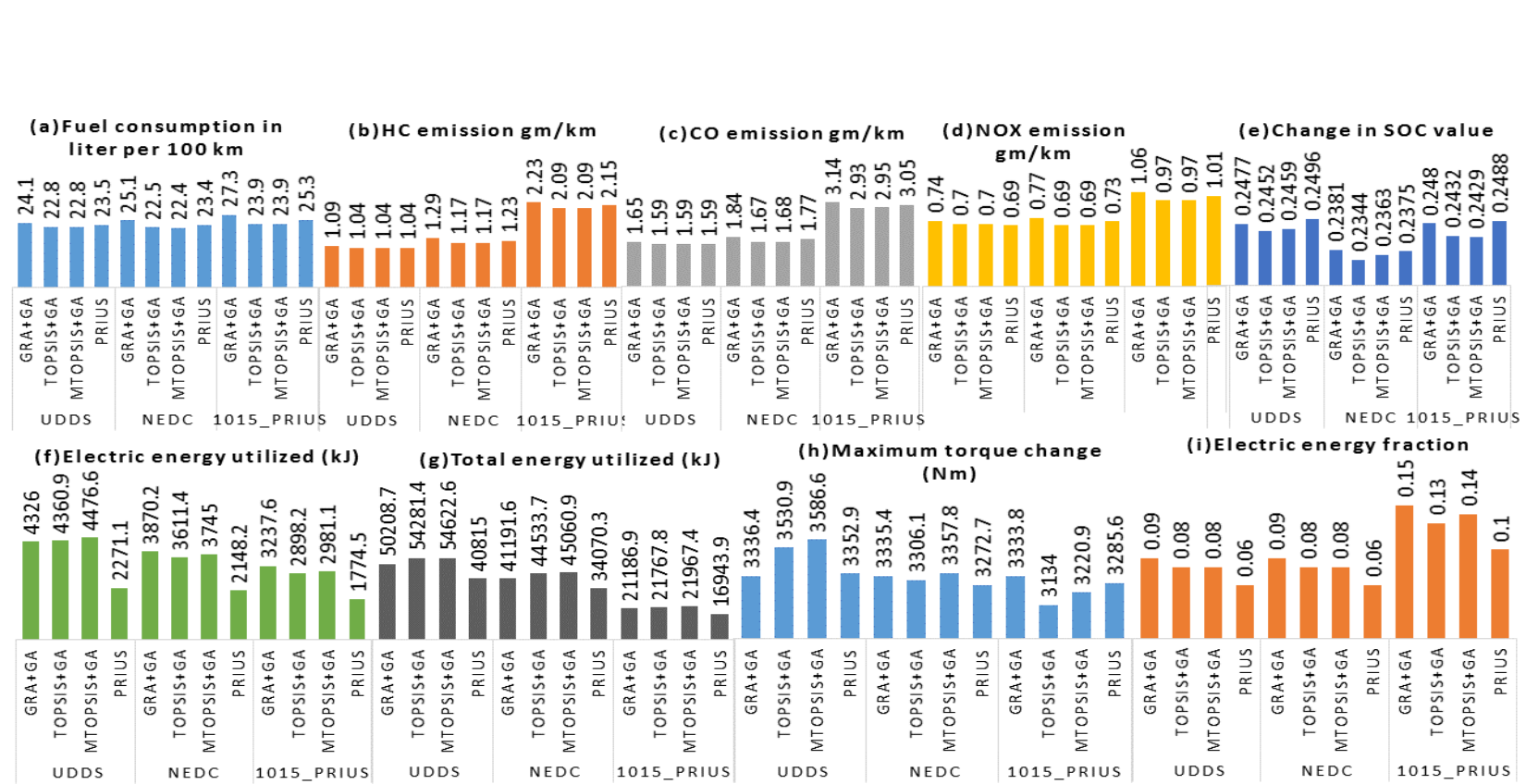


Figure 12. Result of simulation in 25% grade for three different driving cycles (a) fuel consumption (b) HC emission (c) CO emission (d) NOX emission (e) Change in SOC (f) Electric energy utilised (g) Total energy utilised (h) Maximum torque change (i) Electric energy fraction

Table 14. Electric energy fraction in varying road grade (a) Electric energy fraction in UDDS (b) Electric energy fraction in NEDC (c) Electric energy fraction in 1015_6Prius

Driving Cycle	Design	<i>Electric energy fraction</i>		
		0% road grade	10% road grade	20% road grade
UDDS	GRA+GA	0.38	0.36	0.5
	TOPSIS+GA	0.42	0.36	0.6
	MTOPSIS+GA	0.44	0.36	0.59
	Prius or Base model	0.29	0.24	0.37
NEDC	GRA+GA	0.21	0.17	0.32
	TOPSIS+GA	0.18	0.16	0.28
	MTOPSIS+GA	0.18	0.16	0.28
	Prius or Base model	0.13	0.12	0.24
1015 Prius	GRA+GA	0.09	0.08	0.14
	TOPSIS+GA	0.08	0.07	0.13
	MTOPSIS+GA	0.09	0.07	0.14
	Prius or Base model	0.06	0.06	0.11

In prius model the battery capacity is lowest and hence it have lowest capability of supplying the electric energy. This difference between the battery energy storage capability can be found in table 12. Also the obtained design solutions have higher generator power , which helps to recover energy during driving and hence the base model have higher difference between the initial and final SOC value.

The savings are calculated for the four road gradient values and is used to calculate the Total Cost of Ownership (TCO) for five years⁵³. The annual fuel consumption on the basis of travel of 15000 km per year⁵³ has been assessed for translating into cost forming a component in TCO, considering the price of gasoline at \$3 per gallon to in the first year escalating 5% annually and for electric fuel it is at \$0.12 per kWh to escalate in the similar manner. Now, the TCO is expressed as Eq.49⁵³.

$$(49)$$

TCO = Total Cost of ownership = Purchasing price; P_r = resell price at the end of the ownership period;
 C_f = Total fuel cost during the cost of ownership; P = amount borrowed ; N = Number of monthly interest payments; r = monthly interest rate; IC = Insurance Cost; MR = Maintenance and repairs; T = Government tax; S = Government subsidies.

In TCO computation the cost other than the variable one are retrieved from literature and accordingly the repair and maintenance stand at 10%⁵⁶, insurance cost is considered as \$20/month⁵⁴, tax is considered as 10% and the subsidy is \$2500⁵⁴ and Resell value (price) after five years get reduced to 40% of the initial price⁵⁶. It may be noted here that the considered increase in gasoline may actually not materialised for a couple of year according to some assessment ⁵⁷; such changes however will get neutralised if it is considered that the product development will also take time and is likely to be more or less the same. Thereafter the gasoline price will again shoot up and so is factored in the computation. The TCOs, evaluated from SAEA solutions along with the ADVISOR date of the base model are presented in table 15. The changes in TCOs, with respect to the base model along with the variation in fuel cost reduction, emission reduction and gradeability is presented in table 16.

Table 15. Total Cost of Ownership calculation over five years

Solutions	(\$)	(\$)	I_c (\$)	MR (\$)	T (\$)	S (\$)	(\$)	TCO (\$)
GRAGA	27355	17950	12000	2920	2736	2500	4636	29197
TOPSI+GA	27457	18017	12000	2937	2746	2500	4748	29371
MTOPSIS+G A	27803	18244	12000	2949	2780	2500	4699	29487
BASE or Prius	25000	16405	12000	3604	2500	2500	11839	36048

Table 16. Model comparison summary

	Fuel cost reduction	Emission reduction			Total cost of ownership reduction	θ%
		HC	CO	NOX		
GRA+GA	60.84%	23.32%	22.92%	19.35%	19.00%	19%

TOPSI+GA	59.90%	20.46 %	20.83 %	18.11%	18.52%	24%
MTOPSIS+GA	60.30%	20.46 %	21.35 %	18.11%	18.20%	25%

Table 16 shows a distributed improvement in features across the three design or their modelling, therefore ranking has been required to select the preferred solution methodology in design and for this purpose, multicriteria decision making method with weighted sum⁵⁸ approach has been utilised. It has been evaluated with varying weightage emission and gradeability as the fuel cost reduction and TCO reduction does not exhibits any appreciable difference for these three models. For MCDM application, the weight of the two stated entities, namely emission reduction and gradeability are chosen with varying weight from 0.3 to 0.7 for either factor. The emission which is chosen as a criterion for MCDM comprising of HC, CO and NOX to be in a proportion 1:1.3:4 of as observed in a research article ⁵⁶. These results have been presented in figure 13 and discussed in the next section.

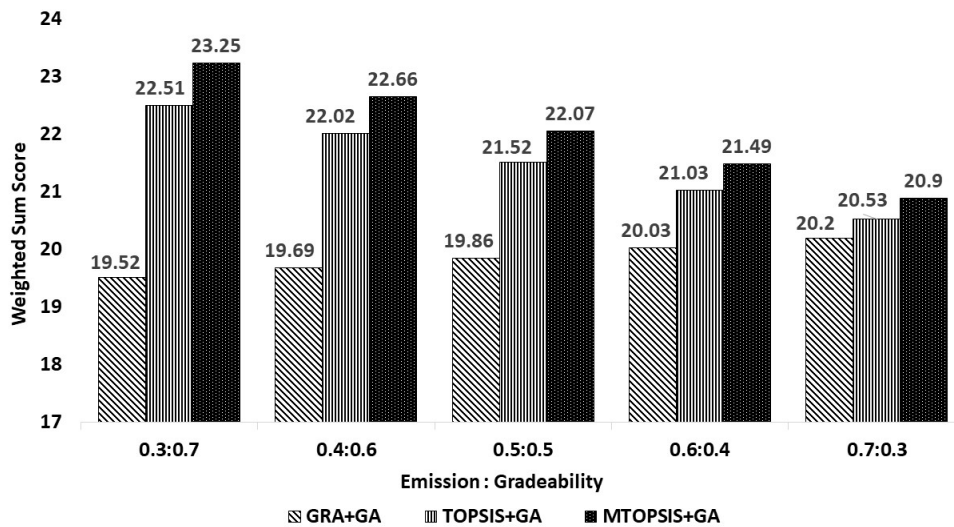


Figure 13. Weighted sum score for three SAEA solutions

Results discussion

In the analysis of variance, in table 4, 8 and 10, shows that the $P_{\max\text{eng}}$, N_{bat} , N_r , N_s and i_0 are the most important parameters as the p values are less than 0.05 for all eleven parameters. It indicates that the change in engine, battery and transmission have significant influence while increasing the vehicle power or designing a powerful PHEV satisfying the criteria or objectives related to ecodesign and vehicle performance used in this study. The optimisation results in table 12 show an increment in the size of engine power, battery energy and generator power for all designs. However, in case of motor power value, all the design points, except GRA variant, are increased. The possible reason is to increase the wheel power supply. However, the increased energy of the battery module with no variation in the number of battery module shows the increased storage capacity for the individual battery.

It can be observed, in table 8 through 11, that the variation in road gradient for the same driving pattern have an effect on fuel consumption and energy consumption. It shows that the increase in driving on the higher gradient value leads to a decrease in fuel economy (FE). Also, in higher road gradient value, the utilisation of electric energy has been increased as intended by all the SAEA based design solutions because of the extra power demand due to increase in gradeability. The total cost of ownership (TCO) analysis and the summary of model performance has been presented in table 15 and 16, respectively, for the three design solution points obtained from three surrogate assisted optimisation algorithms. The result in table 16, shows that the SAEA models reduce the total fuel cost by about 60 % over the ownership period or conventionally considered life of the vehicle in comparison to the base model. The emission values also reduced in comparison to the base model and here GRA based SAEA solution produces better result while in terms of gradeability the MTOPSIS based SAEA is the best solution which can be observed in table 16. In the final weighted sum approach for best design selection, it has been observed, in figure 13, the MTOPSIS based SAEA produces the best result in the wide range of variation weight value. MTOPSIS based SAEA solution achieved the grade compatibility through enhancing the maximum power of traction sources. The engine power, motor power and generator power are enhanced by 6 kW, 18kW and 8kW respectively. Also, the battery energy capacity has been increased by 2.66 kWh. The result shows that the reduction in TCO value is 18.20% and emission is reduced on average around 20%. Further it may be noted lightweighting of the vehicle is materialising from all three aforesaid SAEA solutions and their magnitudes are 9.09 %, 7.42 % and 6.36% for the model hybridised with GRA, TOPSIS and MTOPSIS techniques respectively. However for satisfying

the conditions of the objectives particularly the vehicles capability to travel in rolling terrain at the prescribed speed level which is being attained by MTOPSIS-SAEA model and the corresponding lightweighting is by 6.36 % which well above 6 %.

Conclusions

The proposed methodology for PHEV powertrain design optimisation combining ecodesign and vehicle operating performance factors exhibits improvement in the attributes under both these categories, while the GHG emission has reduced by around 20% where the fuel consumption has substantially reduced by 60% during the useful life of the vehicle. Since here the focus is on Gradeability extending to rolling terrain, a salient consideration for design, getting satisfied through MTOPSIS-SAEA modelling, the corresponding lightweighting of 6.36%, that is well over 6 percent would be considered as practicable. The design is capable to scale the rolling terrain at the recommended optimal speed of the vehicle. The comparison analysis amongst alternative optimisation methodologies has ascertained the most suitable one through the analysis of performance providing guidance for the use of such in design methodology. Therefore, the proposed methodology can be gainfully implemented in the design of the powertrain in a HEV in passenger car category.

Abbreviation

<i>ADVISOR</i>	Advance Vehicle Simulation Software	<i>Li-ion</i>	Lithium-ion battery
<i>ANOVA</i>	Analysis of Variance	<i>MTOPSIS</i>	modified TOPSIS
<i>CO</i>	Carbon-Monoxide	<i>MTC</i>	Maximum Torque Change
<i>CAPSO</i>	Chaos-enhanced Accelerated Particle Swarm Optimization	<i>MCDM</i>	Multi-Criteria Decision Making
<i>DF</i>	Digrees of Freedom	<i>NEDC</i>	New European Driving CYcle
<i>DOE</i>	Design of Experiment	<i>NIS</i>	Negative Ideal Solution
<i>EB</i>	Energy Based	<i>NREL</i>	National Renewable Energy Laboratory
<i>EEU</i>	Electric Energy Utilised	<i>OAD</i>	Orthogonal Array Design
<i>FTP</i>	Federal Test Procidure	<i>PHEV</i>	Plugin Hybrid Electric Vehicle
<i>FC</i>	Fuel consumption	<i>PMS</i>	Power Management System
<i>GA</i>	Genetic Algorithm	<i>PIS</i>	Positive Ideal Solution

<i>GRA</i>	Grey Relational Analysis	<i>SAE</i>	Society of Automotive Engineers
<i>GHG</i>	Green House Gas	<i>SOC</i>	State of Charge
<i>GRG</i>	Grey relational grade	<i>TOPSIS</i>	Technique for Order Preference by Similarity to Ideal Solution
<i>HC</i>	hydrocarbon	<i>TEU</i>	Total Energy Utilised
<i>HWFET</i>	Highway Fuel Economy Test	<i>UDDS</i>	Urban Dynamometer driving cycle
<i>J1634</i>	EV Energy Consumption and Range Test Procedure	<i>1015_6Prius</i>	Toyota Prius testing driving cycle
<i>LP</i>	Linear Program		

Symbols

	Vehicle front area		Motor input power
	Acceleration		Engine Maximum Power
	Positive Ideal Solution and Negative Ideal Solution		Maximum motor power
a_{max}	Maximum vehicle linear acceleration		Closeness coefficient
	Aerodynamic drag coefficient		Distance between alternatives
	Carbon emission		Tire radius
	Maximum charge	T	Temperature
	Used charge		Vehicle linear velocity
,	Euclidian distance from the positive and negative ideal solution	V_{max}	Maximum vehicle linear velocity
del_{soc}	State of charge change		Weighted normalised matrix
E_L	Distance failed to travel		Weighted normalised matrix element
E_v	Velocity error		Weight
E_a	Acceleration error	x	variable
	Carbon emission function		Normalised limit of response value
	Hydrocarbon emission function	y_i^0	Response value
	Nitrox emission function		Percentage value of road grade
	Motor power function		Mass change
	Fuel consumption function		Deviation coefficient
	Rolling coefficient		Engine power scale factor
	Inertia function	ϵ	Fraction of electric energy utilised
FE	Fuel Economy		Motor torque scale factor
	Gravitational acceleration		Engine speed scale factor
	Hydrocarbon emission from engine		Generator mass scale factor
	Gear mechanism ratio		Motor power scale factor
	Finaldrive gear ratio		Engine torque scale factor
I	current		Motor rotational velocity scale factor
	Ratio of ring gear teeth and sun gear teeth number		Gray relational coefficient
	Engine inertia		Air density
	Ratio of Ring teeth number to Sun teeth number		Vehicle powertrain efficiency
	Motor mass		Efficiency of motor
	Vehicle mass		Generator efficiency
	Engine mass		Powersplit efficiency
	Battery mass		Final drive efficiency
m, n	Limit variable		Road slope angle
	Number of battery module		Brake torque on the wheel
	Teeth number of Ring gear		Engine torque

Teeth number of Sun gear
 Nitrox emission from engine
 Elements of decision matrix
 Maximum power of generator
 Generator power
 Motor power
 Generator power output
 Engine power
 Motor output power
 Motor power Loss

Motor torque
 Motor torque
 Generator torque
 Wheel torque
 Output rotational velocity
 Engine rotational velocity
 Motor rotational velocity
 Generator rotational velocity
 Motor rotational velocity
 Gray coefficients

References

1. Yi C, Epureanu BI, Hong SK, Ge T, Yang XG. Modeling, control, and performance of a novel architecture of hybrid electric powertrain system. *Applied Energy*. 2016 Sep 15;178:454-67.
2. Li J, Jin X, Xiong R. Multi-objective optimisation study of energy management strategy and economic analysis for a range-extended electric bus. *Applied energy*. 2017 May 15;194:798-807.
3. Huang Y, Wang H, Khajepour A, Li B, Ji J, Zhao K, Hu C. A review of power management strategies and component sizing methods for hybrid vehicles. *Renewable and Sustainable Energy Reviews*. 2018 Nov 1;96:132-44.
4. Herrera V, Milo A, Gaztañaga H, Etxeberria-Otadui I, Villarreal I, Camblong H. Adaptive energy management strategy and optimal sizing applied on a battery-supercapacitor based tramway. *Applied Energy*. 2016 May 1;169:831-45.
5. Chambon P, Curran S, Huff S, Love L, Post B, Wagner R, Jackson R, Green Jr J. Development of a range-extended electric vehicle powertrain for an integrated energy systems research printed utility vehicle. *Applied Energy*. 2017 Apr 1;191:99-110.
6. Murgovski N, Marinkov S, Hilgersom D, de Jager B, Steinbuch M, Sjöberg J. Powertrain sizing of electrically supercharged internal combustion engine vehicles. *IFAC-PapersOnLine*. 2015 Jan 1;48(15):101-8.
7. Yang Y, Hu X, Pei H, Peng Z. Comparison of power-split and parallel hybrid powertrain architectures with a single electric machine: Dynamic programming approach. *Applied energy*. 2016 Apr 15;168:683-90.
8. Qin Z, Luo Y, Zhuang W, Pan Z, Li K, Peng H. Simultaneous optimisation of topology, control and size for multi-mode hybrid tracked vehicles. *Applied energy*. 2018 Feb 15;212:1627-41.
9. Dimitrova Z, Maréchal F. Techno-economic design of hybrid electric vehicles and possibilities of the multi-objective optimisation structure. *Applied energy*. 2016 Jan 1;161:746-59.

10. Zhou Q, Zhang W, Cash S, Olatunbosun O, Xu H, Lu G. Intelligent sizing of a series hybrid electric powertrain system based on Chaos-enhanced accelerated particle swarm optimisation. *Applied Energy*. 2017 Mar 1;189:588-601.
11. Zhou X, Qin D, Hu J. Multi-objective optimisation design and performance evaluation for plugin hybrid electric vehicle powertrains. *Applied Energy*. 2017 Dec 15;208:1608-25.
12. Cai Y, Ouyang MG, Yang F. Impact of power split configurations on fuel consumption and battery degradation in plugin hybrid electric city buses. *Applied energy*. 2017 Feb 15;188:257-69.
13. Zhang Y, Zhao H, Huang K, Qiu M, Geng L. Hybrid optimisation and its applications for multi-mode plugin hybrid electric vehicle. *Proceedings of the Institution of Mechanical Engineers, Part D: Journal of Automobile Engineering*. 2020 Jan;234(1):228-44.
14. Madanipour V., Montazeri-Gh M., Mahmoodi-k M., Multi-objective component sizing of plugin hybrid electric vehicle for optimal energy management. *Clean Technologies and Environmental Policy*. 2016;18: 1189–1202.
15. Millo F, Cubito C, Rolando L, Pautasso E, Servetto E. Design and development of an hybrid light commercial vehicle. *Energy*. 2017 Oct 1;136:90-9.
16. Holjevac N, Cheli F, Gobbi M. Multi-objective vehicle optimisation: Comparison of combustion engine, hybrid and electric powertrains. *Proceedings of the Institution of Mechanical Engineers, Part D: Journal of Automobile Engineering*. 2020 Feb;234(2-3):469-87.
17. Geng S, Meier A, Schulte T. Model-based optimisation of a plugin hybrid electric powertrain with multimode transmission. *World Electric Vehicle Journal*. 2018 Jun;9(1):12.
18. He Y., Wang C., Zhou Q., Li J., Makridis M., Williams H., Lu G., Xu H. Multiobjective component sizing of a hybrid ethanol-electric vehicle propulsion system. *Applied Energy*, 2020;266; 114843.
19. Zulkefli M.A.M., Sun Z. Fast Numerical Powertrain Optimization Strategy for Connected Hybrid Electric Vehicles. *IEEE Transactions on Vehicular Technology*, 2019;38:9;8629-8641.
20. Anselma P.G., Niutta C.B., Mainini L., Belingardi G. Multidisciplinary design optimization for hybrid electric vehicles: component sizing and multi-fidelity frontal crashworthiness. *Structural and Multidisciplinary Optimization*, 2020;62:4;2149-2166.
21. Kim J, Kim G, Park YI. Component Sizing of Parallel Hybrid Electric Vehicle Using Optimal Search Algorithm. *International Journal of Automotive Technology*. 2018 Aug 1;19(4):743-9.
22. Qin Z, Luo Y, Li K, Peng H. Optimal design of single-mode power-split hybrid tracked vehicles. *Journal of Dynamic Systems, Measurement, and Control*. 2018 Oct 1;140(10).

23. Pourabdollah M, Egardt B, Murgovski N, Grauers A. Convex optimisation methods for powertrain sizing of electrified vehicles by using different levels of modeling details. *IEEE Transactions on Vehicular Technology*. 2017 Oct 27;67(3):1881-93.
24. Angerer C, Felgenhauer M, Eroglu I, Zähringer M, Kalt S, Lienkamp M. Scalable Dimension-, Weight- and Cost-Modeling for Components of Electric Vehicle Powertrains. In 2018 21st International Conference on Electrical Machines and Systems (ICEMS) 2018 Oct 7 (pp. 966-973). IEEE.
25. Luján JM, Guardiola C, Pla B, Reig A. Cost of ownership-efficient hybrid electric vehicle powertrain sizing for multi-scenario driving cycles. *Proceedings of the Institution of Mechanical Engineers, Part D: Journal of Automobile Engineering*. 2016 Feb;230(3):382-94.
26. Song Z, Zhang X, Li J, Hofmann H, Ouyang M, Du J. Component sizing optimisation of plugin hybrid electric vehicles with the hybrid energy storage system. *Energy*. 2018 Feb 1;144:393-403.
27. Song Z, Hofmann H, Li J, Han X, Ouyang M. Optimization for a hybrid energy storage system in electric vehicles using dynamic programming approach. *Applied Energy*. 2015 Feb 1;139:151-62.
28. Guo H, Sun Q, Wang C, Wang Q, Lu S. A systematic design and optimisation method of transmission system and power management for a plugin hybrid electric vehicle. *Energy*. 2018 Apr 1;148:1006-17.
29. Madanipour V, Montazeri-Gh M, Mahmoodi-k M. Optimization of the component sizing for a plugin hybrid electric vehicle using a genetic algorithm. *Proceedings of the Institution of Mechanical Engineers, Part D: Journal of Automobile Engineering*. 2016 Apr;230(5):692-708.
30. Song Z, Hou J, Xu S, Ouyang M, Li J. The influence of driving cycle characteristics on the integrated optimisation of hybrid energy storage system for electric city buses. *Energy*. 2017 Sep 15;135:91-100.
31. Yang Y, Pei H, Hu X, Liu Y, Hou C, Cao D. Fuel economy optimisation of power split hybrid vehicles: A rapid dynamic programming approach. *Energy*. 2019 Jan 1;166:929-38.
32. Roy HK, McGordon A, Jennings PA. Reducing the variability of hybrid electric vehicle fuel economy in the real world. *Proceedings of the Institution of Mechanical Engineers, Part D: Journal of Automobile Engineering*. 2016 Jul;230(8):1121-30.
33. Dagci OH, Peng H, Grizzle JW. Hybrid electric powertrain design methodology with planetary gear sets for performance and fuel economy. *IEEE Access*. 2018 Jan 23;6:9585-602.
34. Wang Y, Wang X, Sun Y, You S. Model predictive control strategy for energy optimisation of series-parallel hybrid electric vehicle. *Journal of cleaner production*. 2018 Oct 20;199:348-58.
35. Brooker, A. et al., 20113. *ADVISOR Advanced Vehicle Simulator*. [Online] Available at: <http://adv-vehicle-sim.sourceforge.net/> [Accessed 3 March 2019].

36. Francfort J, Karner D, Harkins R, Tardiolo J. Hybrid Electric Vehicle End-Of-Life Testing On Honda Insights, Gen I Civics And Toyota Gen I Priuses. Idaho National Laboratory (INL); 2007 Feb 1.
37. Bhattacharjee D, Bhola P, Dan PK. A Fuzzy Based Propulsion Selection for Fuel Efficiency in Hybrid Electric Vehicle. In ASME 2018 International Design Engineering Technical Conferences and Computers and Information in Engineering Conference 2018. American Society of Mechanical Engineers Digital Collection.
38. Julong D. Introduction to grey system theory. *The Journal of grey system*. 1989 Jan;1(1):1-24.
39. Hwang, C. L. & Yoon, K., 1981. *Multiple Attribute Decision Making: Methods and Applications A State-of-the-Art Survey*. 1 ed. Heidelberg: Springer-Verlag.
40. Ren L, Zhang Y, Wang Y, Sun Z. Comparative analysis of a novel M-TOPSIS method and TOPSIS. *Applied Mathematics Research eXpress*. 2007 Jan 1;2007.
41. Westermann P, Evins R. Surrogate modelling for sustainable building design-A review. *Energy and Buildings*. 2019 May 29.
42. Singh P, Couckuyt I, Elsayed K, Deschrijver D, Dhaene T. Shape optimisation of a cyclone separator using multi-objective surrogate-based optimisation. *Applied Mathematical Modelling*. 2016 Mar 1;40(5-6):4248-59.
43. Iuliano E. Global optimisation of benchmark aerodynamic cases using physics-based surrogate models. *Aerospace Science and Technology*. 2017 Aug 1;67:273-86.
44. Koziel S, Sigurdsson AT. Multi-fidelity EM simulations and constrained surrogate modelling for low-cost multi-objective design optimisation of antennas. *IET Microwaves, Antennas & Propagation*. 2018 Jun 27;12(13):2025-9.
45. Mifsud D, Verdin PG. Surrogate-Based Design Optimisation Tool for Dual-Phase Fluid Driving Jet Pump Apparatus. *Archives of Computational Methods in Engineering*. 2019 Nov 22:1-37.
46. Sun, H., Ge, Y., Lu, W. & Liu, Z., 2019. Geometric optimisation of two-stage thermoelectric generator using genetic algorithms and thermodynamic analysis. *Energy*, Volum 171, pp. 37-48.
47. Cai G, Liang Y, Liu Z, Liu W. Design and optimisation of bio-inspired wave-like channel for a PEM fuel cell applying genetic algorithm. *Energy*. 2020 Feb 1;192:116670.
48. Wang S, Xiao B, Ge Y, He L, Li X, Liu W, Liu Z. Optimisation design of slotted fins based on exergy destruction minimisation coupled with optimisation algorithm. *International Journal of Thermal Sciences*. 2020 Jan 1;147:106133.

49. Wieczorek M, Lewandowski M. A mathematical representation of an energy management strategy for hybrid energy storage system in electric vehicle and real time optimisation using a genetic algorithm. *Applied energy*. 2017 Apr 15;192:222-33.
50. Bhattacharjee D, Ghosh T, Bholra P, Martinsen K, Dan PK. Data-driven surrogate assisted evolutionary optimisation of hybrid powertrain for improved fuel economy and performance. *Energy*. 2019 Sep 15;183:235-48.
51. Wu X, Cao B, Li X, Xu J, Ren X. Component sizing optimisation of plugin hybrid electric vehicles. *Applied energy*. 2011 Mar 1;88(3):799-804.
52. Manual of Specifications and Standards, 2007.
53. Hagman J, Ritzén S, Stier JJ, Susilo Y. Total cost of ownership and its potential implications for battery electric vehicle diffusion. *Research in Transportation Business & Management*. 2016 Mar 1;18:11-7.
54. themoneycalculator, 2020. Toyota Prius Depreciation Calculator. [Internet] Available at: <https://www.themoneycalculator.com/vehicle-finance/calculators/car-depreciation-by-make-and-model/TOYOTA/PRIUS/> [Funnet 25 April 2020].
55. Palmer k, Tate JE, Wadud Z, Nellthorp J. Total cost of ownership and market share for hybrid and electric vehicles in the UK, US and Japan. *Applied Energy*. 2018;209:108-119.
56. eia, 2020. PETROLEUM & OTHER LIQUIDS. [Internet] Available at: <https://www.eia.gov/dnav/pet/hist/LeafHandler.ashx?n=pet&s=emm epm0 pte nus dpg&f=m> [25 April 2020].
57. Triantaphyllou, E. *Multi-Criteria Decision Making: A Comparative Study*. Dordrecht, The Netherlands: Kluwer Academic Publishers (now Springer), p320, 2000.
58. Sakthivel G, Sivakumar R, Ilangkumaran M, Ikua BW. Selection of optimum fish oil fuel blend to reduce the greenhouse gas emissions in an IC engine—A hybrid multiple criteria decision aid approach. *International Journal of Green Energy*, 2016;13:14;1517–1533.